

Chapter One

Introduction

Importance of studying the nonlinear dynamic of Homoclinic chaos using semiconductor lasers and opt couplers is to obtain synchronization in devices that match with current telecommunication technologies and to investigate analogies with collective brain dynamics. The synchronization of spike trains of many individual neurons is the basis of coherent perception. In presence of different external stimuli, different clusters of synchronized neurons are present within the same cortical area. The crucial fact is the dissipation of information. This means that a reading sensitive to (m) collective clusters has lost the detailed information of the (N) components. Information loss means that coding at a higher hierarchical level is not just a computational task, but it violates the procedure of a Turing machine. So we study theoretically the existence of slow chaotic spiking sequences in the dynamics of semiconductor devices with coupled optoelectronic feedback. The detected timescale of this dynamic is fully determined by the high-pass filter in the feedback loop and their erratic, though deterministic, nature is proved by means of the inter-spike interval (ISI) probability distribution. The introduction of an AC-feedback optoelectronic loop adds both third degree of freedom and third much slower time-scale.

The expected result of an incomplete Homoclinic scenario that a saddle-focus could be occurred. For technological applications semiconductor lasers are promising systems to implement secure communication schemes using chaos synchronization, because they exhibit fast dynamics, cheap and one could utilize the existing telecommunication infrastructure for these lasers. However,

due to the fast dynamics of lasers, propagation distances of already a few meters introduce non-negligible delay times in the coupling.

The synchronization of delay-coupled systems in general and delay-coupled lasers in particular has therefore been a focus of research in nonlinear dynamics in recent decades. When lasers are coupled all optically, not only the delay effect is important, but also the optical coupling phases of coherently coupled electric fields are important. Coherent coupling may result in constructive or destructive interference of incoming signals. When the lasers are synchronized, this interference can occur even if the coupling distance is much larger than the coherence length of the beams.

1.1 Literature review

Many efforts of the scientists in the field of chaos generation and nonlinear dynamic of laser had been demonstrated in decade. Fischer, A.P. et al,(2000) illustrated solution to control the dynamical space that is available to the laser, providing a mechanism for controlling its dynamical behavior. Through the use of filters which achieved via a suitable choice of only two parameters. Allaria, E. et al, (2001) reported Homoclinic chaos characterization by regular geometric orbits occurring at erratic times. Phase synchronization at the average repetition frequency was achieved by a tiny periodic modulation of a control parameter. An experiment has been carried on a (CO₂) laser with feedback, set in a parameter range where Homoclinic chaos occurs. Any offset of the modulation frequency from the average induces phase slips over long times. Tang, S. and Liu, J.M. (2003) published experimentally the chaos synchronization in semiconductor laser with delayed optoelectronic feedback. He driven oscillation was not observed in that optoelectronic feedback system

when the coupling strength was increased to a level higher than the feedback strength. Larger, L. et al, (2005) demonstrated a new transition scenario for the general class of delay differential dynamics, from continuous to discrete time behavior. This transition scenario differs from the singular limit map, or adiabatic approximation model that usually considered. The transition from the map to the flow was observed when increasing the pulse repetition rate. The mechanism of that transition opens the way to new interpretations of the general properties of delay differential dynamics, which are universal features of many other scientific domains. From this work the nonlinear delay oscillator architecture presented, will have significant applications in chaotic communication systems. Sprott, J.C. (2007) the simplest chaotic delay differential equation with a sinusoidal non linearity, including the route to chaos, Lyapunov exponent spectrum, and chaotic diffusion. It is prototypical of many other high-dimensional chaotic systems have shown. Arecchi, F.T. et al,(1987) published Successive transitions from Hopf bifurcation to Shilnikov chaos where regular spiking are observed in a laser with feedback when increasing a control parameter. K.Lu and Q.Wang, (2008) presented the chaotic behavior of ordinary differential equations with a homo clinic orbit to a dissipative saddle point under an unbounded random forcing driven by a Brownian motion. The result is then applied to the randomly forced Duffing equation and the pendulum equation. AL-Naimee, K. et al, (2009) demonstrated experimentally and theoretically the existence of slow chaotic spiking sequences in the dynamics of a semiconductor laser with ac-coupled optoelectronic feedback. The timescale of these dynamics was fully determined by the high-pass filter in the feedback loop and their erratic, they found that this

was leads of an incomplete homo clinic scenario to a saddle-focus, where an exact homo clinic connection does not occur. Li, Y., et al, (2010) reported experimentally the time-delay signature (TDS) of chaos in the variable polarization fiber Bragg grating feedback (VPFBGF)- vertical cavity surface emitting laser(VCSEL) is evaluated and then the influences of the operation parameters on the TDS of chaos are analyzed. The results show that the TDS of chaos can be suppressed efficiently through selecting suitable coupling coefficient and feedback rate of the fiber Bragg grating (FBG), and is weaker than that of chaos generated by traditional variable-polarization mirror feedback VCSELs (VPMF-VCSELs) or polarization-preserved FBG feedback VCSELs (PPFBGF-VCSELs). Al-Naimee, K. et al, (2010) published theoretically the dynamics of a semiconductor laser with AC-coupled nonlinear optoelectronic feedback has been experimentally studied. A period doubling sequence of small periodic and chaotic attractors was observed, each of them displaying excitable features. That scenario was found also in a simplified physical model of the system, thus extending the concept of excitability, usually associated to fixed points, also to the case of higher-dimensional attractors. El-Dessoky, M.M. and Yassenl, M.T. (2012) presented and investigated the problem of chaos control and synchronization for new chaotic dynamical system and proposes a simple adaptive feedback control method for chaos control and synchronization under a reasonable assumption. Numerical simulations were shown to verify the analytical results. Flunkert, V. (2012) explained the variety of synchronized motion in coupled chaotic systems applications; for example to increase the power of lasers, to synchronize the output of electronic circuits, to control oscillations in chemical reactions or to

encode electronic messages to secure communications.

1.2 Aims of the study

The objectives of this work are: To present a theoretical model, explaining the existence of chaotic spiking sequences in the dynamics of semiconductor devices with ac-coupled optoelectronic feedback (OEFB) with amplitude modulation. To generate chaos by using directly amplitude modulation optoelectronic feedback. To produce fixed spiral dynamic state, periodic state, double periodic state, chaotic state. To find instability of the chaotic system or (Bifurcation diagram). To control synchronization in unidirectional and bidirectional configurations. To investigate the sensitivity of the configuration (unidirectional and bidirectional).

1.3 Thesis Outlines

In chapter one, we gave a brief introduction, literature review and aims of our study. In chapter two, we demonstrated the theoretical back ground, the basic definitions of laser chaos and synchronization, also we discussed the dynamical model and methodology of the case of study and we suggested

Berkeley Madonna and origin software for simulating the chaos generation and synchronization. In chapter three, we demonstrated our results and discussed them. In chapter four gives the conclusion with some recommendations for the future work.

Chapter Two

Theoretical Background

2.1 Lasers

The laser can be considered as one of the most important inventions in the twentieth century. The important characteristic of the laser is coherence, which implies that the photons oscillate similarly in phase. Coherent light sources have outstanding characteristics compared with natural incoherent light, bright intensity output, high photon energy, good directionality, single wavelength, and narrow spectrum bandwidth in order to enable interference (Uchida, A. (2012)). Laser communications offer a viable alternative to radio frequency (RF) communications for inter satellite links and other applications where high-performance links are necessary. High data rate, small antenna size, narrow beam divergence, and a narrow field of view are characteristics of laser communication that offer a number of potential advantages for system design. The high data rate and large information throughput available with laser communications are many times greater than in radio frequency (RF) systems. The small antenna size requires only a small increase in the weight and volume of host vehicle. In addition, this feature substantially reduces blockage of fields of view of the most desirable areas on satellites. The smaller antennas create less momentum disturbance to any sensitive satellite sensors. The narrow beam divergence of affords interference free and secure operation.

2.2 Ikeda Scenario

A laser system with many interacting degree of freedom can be conveniently realized with time delayed feedback, the nonlinear dynamical behavior of

system with time delayed feedback was first investigated theoretically by Ikeda et al in late(1970)(Fischer, I. et al,(1994). Modeling a passive nonlinear ring resonator, externally pumped by laser. Their investigation based on numerical modeling were the generalized to simple delay equation applicable to whole class of delay system. Ikeda Scenario turned out to be paradigm for dynamical behavior of delayed feedback system. The key features of the Ikeda scenario are the occurrence of multistability of periodic or chaotic attractors and the onset of high-dimensional deterministic chaos via attractor merging. Recently, a semiconductor laser (SL) system has been demonstrated to show experimentally the characteristic phenomena of this scenario. The characterization and modeling of high-dimensional states ($N > 5$) with the help of embedding techniques is a fundamental problem due to the requirements on the amount of data and its precision.

2.3 Chaos

From the beginning of laser history, instabilities of laser output are inevitable due to its inherent non linearity (Maiman, (1960); Maiman et al., (1961)), even though many efforts have been made to stabilize laser output for many engineering applications. Most lasers including semiconductor, fiber, solid state, and gas lasers produce temporal and spatial instabilities of laser output at certain operating conditions or with an additional external perturbation. It has been known that these instabilities can be derived from a deterministic rule of laser dynamics, which can be described by using a set of differential rate equations. These types of instabilities have been known as (Deterministic Chaos) and can be distinguished from instabilities due to stochastic or quantum noise (Uchida, A., (2012)). Chaos is generally used to describe disturbance or

turbulence in many situations. The most acceptable definitions of chaos in science is the instabilities derived from a (Deterministic) rule. The term chaos has been used to describe fluctuations or time-varying or (space-varying) irregular phenomena that are governed by a deterministic rule, which can be described by using a set of mathematical equations. Chaos is a counter intuitive concept in the sense that one may find a mathematical rule in irregular fluctuations of complex dynamics. One of the important characteristics of deterministic chaos is known as (sensitive dependence on initial conditions) (Lorenz, 1963). If two chaotic temporal sequences start from very close but slightly different initial conditions, the two sequences behave similarly at the beginning, however, they start to diverge exponentially in time and never show the same behavior again. This characteristic can be quantitatively measured by using the maximum Lyapunov exponent, and the Existence of the positive maximum Lyapunov exponent is a proof of deterministic chaos. A tiny error of the initial conditions makes chaotic irregular sequences unpredictable. This fact implies that chaos is unpredictable for a long-term duration due to the sensitive dependence on initial conditions, although chaos is predictable for a short-term period due to the existence of deterministic rules (Uchida, A., 2012). Chaotic behavior of a dynamic system has a very large (possibly infinite) number of attractors and is sensitive to initial conditions. Sensitivity to initial conditions means that each point in such a system is arbitrarily closely approximated by other points with significantly different future trajectories. Thus, an arbitrarily small perturbation of the current trajectory may lead to significantly different future behavior. The necessary conditions for chaos ($n > 2$, nonlinear, bounded trajectories, continuous-time systems) (n refer to the degree of freedom).

2.4 Chaotic time series in a system

A time series is a sequence of scalar values over time (Zhang, J., et al, 2008) describe a time series as a sequence of regularly sampled quantities out of an observed system. (Kantz, H. and Schreiber, T., 1997) define a time series as a set of scalar values which measures the status of a certain system over time. A time series is the historical record of a system, with the measurements taken at regular intervals with a consistency in the method of measurement and the system (Camiller, M., 2004). It is a useful source of information to analyze and investigate the characteristics and behaviors of a system (Zhang et al, 2008). Being aperiodic, bounded, deterministic and sensitive to initial conditions differentiates chaotic time series from other types of time series (Wilding, R. D., 1998). Time series analysis consists of the techniques to manipulate, characterize and perform quantitative and qualitative analysis to understand the underlying characteristics of a system (Camiller, M., 2004). In analyzing time series, an important step is to determine the characteristics of the data. The following methods have been used to differentiate chaotic data from non-chaotic data. The Lyapunov exponent method which looks for the main characteristics of chaotic systems, sensitivity to initial conditions, is the most preferable method in the literature.

2.4.1 Lyapunov exponent

An important characteristic of chaotic systems which is defined as the butterfly effect, it is the high sensitivity of the system to the initial conditions (A. Wolf, 1985). The largest Lyapunov exponent is the most practical method to identify chaotic behavior in a system. The Lyapunov exponent quantifies the convergence and divergence of neighboring trajectories. If there exists a

function which maps $(x(t) \text{ to } x(t+1))$, $x(t) \rightarrow R(x(t)) = x(t+1)$, for two nearby initial points at x_0 and $(x_0 + \Delta x_0)$ after one iteration the separation of the points can be calculated by equation (2.3)

$$x_{(1)} = R(x_{(0)} + \Delta x_{(0)}) - R(x_{(0)}) \quad (2.1)$$

$$\dot{R} = \frac{dR}{dx} \quad (2.2)$$

The Lyapunov exponent at $x_{(0)}$ can be defined such that:

$$e^\lambda = |x_{(1)}/x_{(0)}| \quad (2.3)$$

Or can be rearranged as shown in Eq. (2.6)

$$\lambda = \ln |\Delta x_{(1)}/\Delta x_{(0)}| \quad (2.4)$$

$$\ln \left| \frac{\Delta x_{(1)}}{\Delta x_{(0)}} \right| \cong \ln |\dot{R}(x_{(0)})| \quad (2.5)$$

The quantity $(\Delta x_{(1)}/\Delta x_{(0)})$ is the Lyapunov exponent or the measurement of the stretching at $x = x_0$. If $(\Delta x_{(1)}/\Delta x_{(0)})$ is negative, it means the two nearby points interchange their order (the larger becomes smaller, and vice versa) upon iteration. To obtain the global Lyapunov exponent, the average of Eq. (2.5) over a large number of iterations is calculated as presented in equation (2.6).

$$\lambda = \lim_{N \rightarrow \infty} \frac{1}{N} \sum_{t=0}^{N-1} \ln |\dot{R}(x(t))| \quad (2.6)$$

The value zero is interpreted as cyclic behavior, a negative exponent means non chaotic behavior, and a positive Lyapunov exponent proves the existence of chaos in the system (Addison, P.S (1997) and Wolf, A., et al(1985).

2.4.2 Fourier transform

Fourier transform can be used to identify chaos in a given time series. The Fourier transform calculates the present frequencies in a time series. Fourier transforms of the time series, $x(t)$, $t = 0, 1, 2, \dots, N-1$, where N is the number of

points can be calculated by equation (2.7).

$$x(k) = \frac{1}{N} \sum_{t=0}^{N-1} x(t) e^{-2\pi i(kT/N)} \quad k = 0, 1, 2, \dots, N-1 \quad (2.7)$$

Where (i) is the imaginary number. The power spectrum is the square of the $X(k)$ and can be calculated by equation (2.8).

$$p(k) = \frac{1}{N^2} \left| \sum_{t=0}^{N-1} x(t) e^{-2\pi i(kT/N)} \right|^2 \quad k = 0, 1, 2, \dots, N-1 \quad (2.8)$$

Plotting the power spectrum of the time series can assist in determining the nature of the time series. The spectrum for chaotic time series will be broadband, meaning that the difference between the highest power value and the lowest value in the power spectrum plot is considerable, with a broad peak, i.e. that a wide range of frequencies are available in the power spectrum plot. Random data should have a constant valued power spectrum. For periodic data, the power spectrum spikes at frequencies that characterize the system and remain close to zero for the others (Addison, P.S., (1997) and Frazier, C. and Kockelman, K., (2004).

2.4.3 Attractor

An attractor is a set of values in the phase space to which a system migrates over time, or iterations. It need more than two dimensional s. Attractors can have as many dimensions as the number of variables that influence its system (Abraham, R. and Ueda, Y.eds (2001). The chaotic attractor in phase space is densely sampled by an infinite number of unstable periodic orbits (Liu, Y. and Ohtsubo, J., (1994). A range of possible attractors can be shown in fig.2.1 (J. Mork, et al, (1992).

2.4.3.1 Attractor types

The attractors can either be: fixed point, which represents a stable constant

output which is a point of a function that does not change under some transformation. A limit cycle is an attractor that is periodic in time, that cycle periodically through an ordered sequence of states, which represents a periodic oscillation. A torus, is an attractor consisting of (N) independent oscillations, plotted in phase space which represent a quasi-periodic output power and chaos, which represents output power fluctuating chaotically called sometimes a strange attractor, is an attractor which it has non-integer dimension , or the dynamics on it are chaotic. The chaotic attractor behaves in a rather different way from fixed state or periodic oscillations. At chaotic oscillations, the state goes around points within the closed compact space in the attractor; it never visits the same point in the space. The trajectory crosses in the attractor

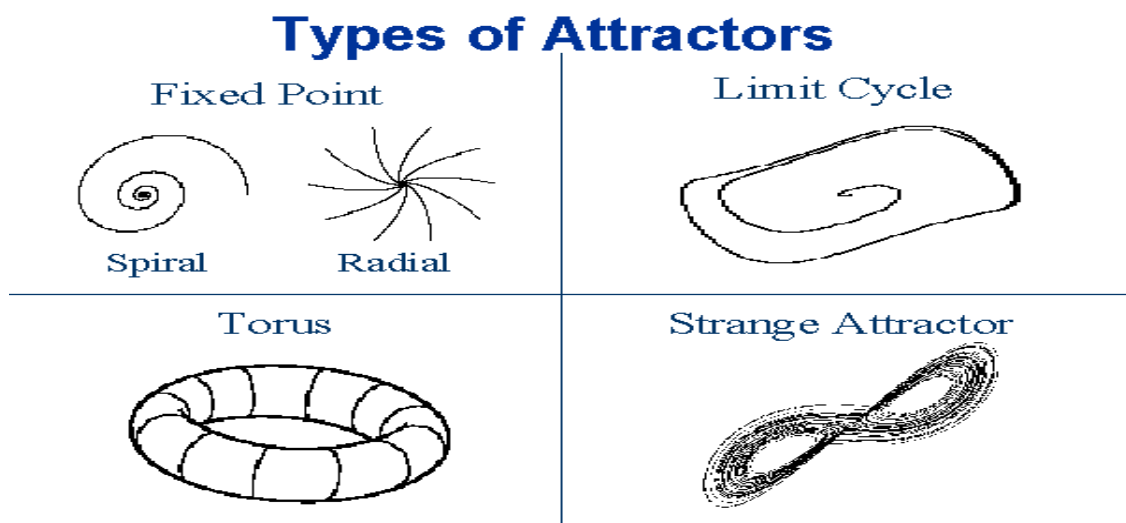


Figure 2.1: The schematic of attractor's type

The chaotic trajectory goes around in a multidimensional space and never crosses in such a space. A chaotic attractor is quite different from other periodic oscillations and looks very strange. Therefore, it is sometimes called a complex or (strange) attractor.

2.4.4 Bifurcation Diagram

A bifurcation is a period doubling change from an (N) point to (2N) point

attractor, which occurs when the control parameter is changed. It is a qualitative change in the behavior (attractor) of a dynamic system associated with a change in control parameter (a control parameter, is a parameter in the equations of a dynamic system), if control parameters are allowed to change, the dynamic system would also change, changes beyond certain values can lead to bifurcations. There are many different bifurcations: saddle-node, Hopf,

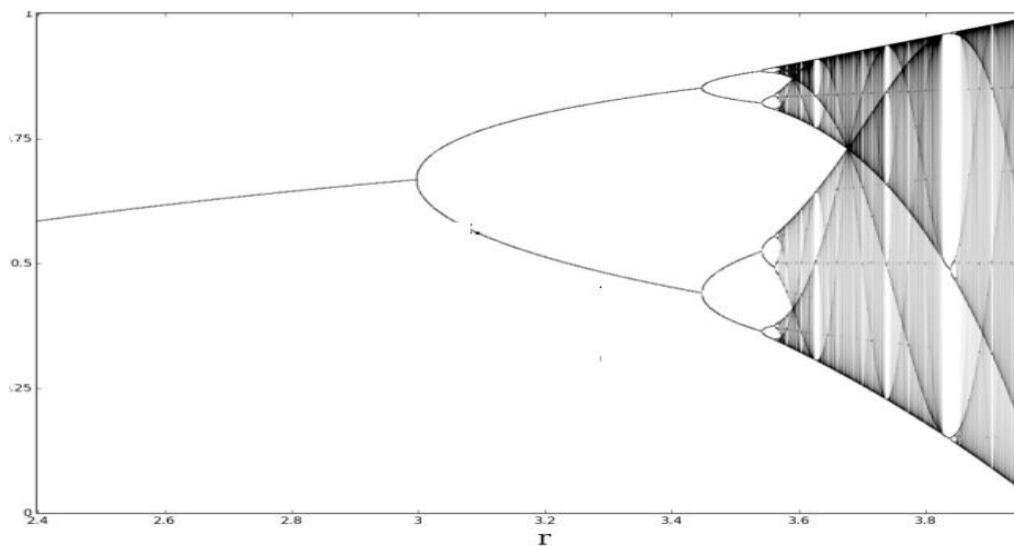


Figure 2.2: The schematic of the logistic map

Bifurcation diagram period doubling and torus. The saddle- node bifurcation is the basic mechanism by which fixed points are created and destroyed, as a parameter is varied.

2.4.5 Shilnikov Homoclinic Chaos and Saddle-focus

Shilnikov Homoclinic orbits are trajectories that depart from a fixed saddle focus point, with specific eigenvalues, and return to it after an infinity time (that is also true to time reversal evolution) (Medrano-T, R.O.,et al (2005)).

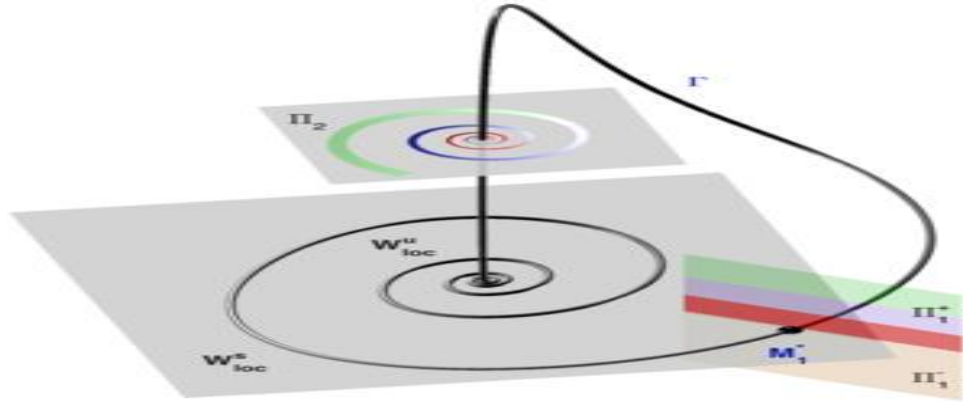


Figure 2.3: Homoclinic loop of a saddle-focus in the Rossler system.

We consider such a saddle-focus at the origin in a 3D system.

$$\dot{x} = -\rho x - \omega y + f_1(x, y, z) \quad (2.1a)$$

$$\dot{y} = \omega x - \rho y + f_2(x, y, z) \quad (2.9b)$$

$$\dot{z} = \gamma z + f_3(x, y, z) \quad (2.9c)$$

Here its Lyapunov characteristic exponents are:

$$\lambda_{1,2} = -\rho \pm i\omega \quad (2.10)$$

$\rho > 0$, $\omega = 0$ and W^u is 1D. The manifold W^u is the union of O and two separatists that tend to

$$\lambda_3 = \gamma > 0 \quad (2.11)$$

Smooth functions F_i , along with their first partials, vanish at the origin. The stable manifold W^s of the saddle-focus O is 2D then, whereas the unstable one W^u is 1D. The manifold W^u is the union of O and two separatists that tend to O as $t \rightarrow \infty$. A homoclinic loop Γ of the saddle-focus is a trajectory bi-asymptotic to O as $t \rightarrow \pm\infty$, Fig.2.3. In other words, $\Gamma \in W^s \cap W^u$.

2.4.6 Distribution of Inter-Spike Intervals (ISI)

The Inter-Spike Intervals is a model for studying the properties of irregular spiking Homoclinic chaos and the dynamics of spiking and bursting in a neuron model. ISI measures time between consecutive spikes. The discrete distribution of ISI decays exponentially and have peaks located at all natural (Reich, D.S.,et

al (2000).

2.5 Lasers and Chaos

The connection between lasers and chaos was made in (1975) (Haken, (1975)), where it was shown that a set of nonlinear differential equations from Maxwell Bloch equations for a laser model resembles Lorenz equations which are the basic model for deterministic chaos. Since then, many observations have been reported in experiments and numerical simulation in the (1980s). It was found that most lasers produce chaotic fluctuations of laser intensity (Uchida, A., (2012).

2.6 The synchronization of chaotic systems

2.6.1 Introduction

Synchronization mean share the common time. The original meaning of synchronization has been maintained up to now in the colloquial use of this word, as agreement or correlation in time of different processes. Historically, the analysis of synchronization phenomena in the evolution of dynamical systems has been a subject of active investigation since the earlier days of physics. It started in the 17th century with the finding of Huygens that two very weakly coupled pendulum clocks (hanging at the same beam) become synchronized in phase (Hugenii, C., et al (1986) Other early found examples are the synchronized lightning of fireflies, or the peculiarities of adjacent organ pipes which can almost reduce to one another to silence or speak in absolute unison. For an exhaustive overview of the classic examples of synchronization of periodic systems we address the reader (Blekman,I.I.,((1988). Recently, the search for synchronization has moved to chaotic systems. In this latter framework, the appearance of collective (synchronized) dynamics is, in general,

not trivial. Indeed, a dynamical system is called chaotic whenever its evolution sensitively depends on the initial conditions. It implies that two trajectories emerging from two different closely initial conditions separate exponentially in the course of the time. As a result, chaotic systems intrinsically defy synchronization, because even two identical systems starting from slightly different initial conditions would evolve in time in an unsynchronized manner. This is a relevant practical problem, in so far as experimental initial conditions are never known perfectly. The setting of some collective (synchronized) behavior in coupled chaotic systems has therefore a great importance and interest. The study of synchronization in coupled chaotic systems, As we will see, not always the word synchronization will be taken as having the same colloquial meaning, and we will need to specify what synchrony means in all particular contexts in which we will describe its emergence. As a preliminary definition, we will refer to synchronization of chaos as a process where in two (or many) chaotic systems (either equivalent or nonequivalent) adjust a given property of their motion to a common behavior, due to coupling or forcing. This ranges from complete agreement of trajectories to locking of phases. The first thing to be highlighted is that there is a great difference in the process leading to synchronized states, depending upon the particular coupling configuration. Namely, one should distinguish two main cases: unidirectional coupling and bidirectional coupling. In the former case, other names were given in the literature of this type of synchronization, such as one-way diffusive coupling, drive-response coupling, and master-slave coupling or negative feedback control. This implies that one subsystem evolves freely and drives the evolution of the other. As a result, the response system is slaved to follow the dynamics of

the drive system, which, instead, purely acts as an external but chaotic forcing for the response system. In such a case external synchronization is produced. Typical examples are communication with chaos (chaos communication). A very different situation is the one described by a bidirectional coupling. Here both subsystems are coupled with each other, and the coupling factor induces an adjustment of the rhythms on to a common synchronized manifold, thus inducing a mutual synchronization behavior. This situation typically occurs in physiology, e.g. between cardiac and respiratory systems or between interacting neurons or in nonlinear optics, e.g. coupled laser systems with feedback. These two processes are very different not only from a philosophical point of view: up to now no way has been discovered to reduce one process to another, or to link formally the two cases.

2.6.2 Types of synchronization

Many different synchronization states have been studied in the past (10)years, namely complete or identical synchronization (CS) (Fujisaka, H., and Yamada, T.,(1983) and Pecora, Louis M., and Carroll, Thomas L.,(1990) phase (PS) (Rosenblum, M. G.,et al (1996) and Rosa,E. R., et al (1998) and lag (LS) synchronization (Rosenblum,M.G., et al (1997) generalized synchronization (GS) (Rulkov,N.F., et al (1995) and Kocarev,L., Parlitz, U.,(1996), intermittent lag synchronization (ILS) (Rosenblum, M.G., et al (1997) and Boccaletti, S., Valladares,D.L.,(2000), imperfect phase synchronization (IPS)(Zaks,M.A.,et al (1999), and almost synchronization (AS)(Femat, R. and Solis-Perales, G.,(1999). (GS) goes further in using completely different systems and associating the output of one system to a given function of the output of the other system (Rulkov,N.F., et al (1995) and Kocarev,L., Parlitz, U.,(1996).

Coupled non identical oscillatory or rotatory systems can reach an intermediate regime (PS), where in a locking of the phases is produced, while correlation in the amplitudes remain weak (Rosa,E.R., et al (1998). The transition to (PS) for two coupled oscillators has been firstly characterized with reference to the Rossler system (Rosa, E.R., et al(1998). (LS) is a step between (PS)and(CS). It implies the asymptotic bounded ness of the difference between the output of one system at time (t) and the output of the other shifted in time of a lag time (τ) lag. This implies that the two outputs lock their phases and amplitudes, but with the presence of a time lag (Rosa, E.R., et al (1998). (ILS)Simplifies that the two systems are most of the time verifying (LS), but intermittent bursts of local non synchronous behavior may occur in correspondence with the passage of the system trajectory in particular attractor regions wherein the local Lyapunov exponent along a globally contracting direction is positive (Rosenblum, M.G.,et al (1997) and Boccaletti, S., and Valladares, D.L.,(2000). Analogously, (IPS) is a situation where phase slips occur within a (PS) regime (Zaks,M.A., et al (1999). Finally, (AS) results in the asymptotic bounded ness of the difference between a subset of the variables of one system and the corresponding subset of variables of the other system (Femat, R. and Solis-Perales, G.,(1999). The first scenario of transition among different types of synchronization was described for symmetrically coupled non identical systems and consisted in successive transitions between (PS, LS) and a regime similar to(CS)when increasing the strength of the coupling (Boccaletti, S.,Valladares, D.L.,(2000).

2.6.3 Synchronization of identical systems (CS)

Complete synchronization (CS) was the first discovered and is the simplest

form of synchronization in chaotic systems. It consists in a perfect hooking of the chaotic trajectories of two systems which is achieved by means of a coupling signal, in such a way that they remain in step with each other in the course of the time. This mechanism was first shown to occur when two identical chaotic systems are coupled unidirectional, provided that the conditional Lyapunov exponents of the subsystem to be synchronized are all negative (Pecora, Louis M. and Carroll, Thomas L., (1990). Chaotic systems are dynamical systems that defy synchronization, due to their essential feature of displaying high sensitivity to initial conditions. As a result, two identical chaotic systems starting at nearly the same initial points in phase space develop onto trajectories which become uncorrelated in the course of the time. Nevertheless, it has been shown that it is possible to synchronize these kinds of systems, to make them evolving on the same chaotic trajectory (Pikovsky, A.S., (1984) and Pecora,L.M., Carroll, T.L.,(1991).

When one deals with coupled identical systems, synchronization appears as the equality of the state variables while evolving in time. This referred to a complete synchronization (CS). Other names were given in the literature, such as conventional synchronization or identical synchronization. In this section, we will discuss main properties of this kind of synchronization. Most of the exposed ideas can be easily extended to discrete systems, such as chaotic mappings. As for the coupling, one has to distinguish between two different situations. When the evolution of one of the coupled systems is unaltered by the coupling, the resulting configuration is called unidirectional coupling or drive response coupling. On the contrary we will refer to bidirectional coupling when both systems are connected in such a way that they mutually influence each

other's behavior. Inside this classification, the appearance and robustness of synchronization states have been established by means of several different coupling schemes, such as the Pecora and Carroll method (Pecora, L.M. and Carroll, T.L., (1990) and He, R., Vaidya, P.V., (1992), the negative feedback (Kapitaniak, T., (1994), the sporadic driving, (Amritkar, R.E., Gupte, N., (1993), the active passive decomposition (Kocarev, L., Parlitz, U. (1995) and Parlitz, U., et al (1996), the diffusive coupling and some other hybrid methods (Gmez, J., and Matas, M. A., (1995). A description and analysis of some different coupling schemes is given in (Wu, C.W. and Chua, L.O., (1994) a single mathematical framework. When one deals with coupled identical systems, synchronization appears as the equality of the state variables while evolving in time. The two synchronization schemes described here and several other drive response configurations have been used into the design of communication devices, which is perhaps the most promising application of synchronized chaotic behavior (Carroll, T.L., and Pecora, L.M., (1993) and Carroll, T.L., (1994). For example, one can have two remote systems behaving chaotically, but synchronized with each other through only one driving signal. A sender can add a given message to the drive, thus masking the information from any third party who wants to intercept it. The receiver can extract the message by using the synchronization error between the drive and the regenerated signal, where the message appears as De synchronization episodes. Other promising applications with chaotic lasers have been proposed. Remote sensing applications with chaotic lasers have been reported as chaotic lidar and radar systems. Blind signal separation using independent component analysis has been applied to chaotic temporal waveforms of laser output for the purpose of multiplexing communications. In

addition, fractal optics have been used for wireless optical communication applications as a chaos mirror (Uchida, A., (2012).

2.6.4 Optical Communication with Synchronized Chaotic Lasers

Synchronization of chaos leads to an important application to optical chaos communications (Uchida, A., 2012). Standard optical communication utilizes optical periodic carrier for encoding and decoding the message and there is no consideration for security in hardware level. Optical chaos communication leads to an additional layer of security or privacy in optical communication by using chaotic temporal carriers. These hardware-dependent optical communication systems have been developed and there have been international projects to implement optical chaos communication systems in real-world optical networks (Uchida, A., 2012).

The technique of synchronization of chaos is used to reproduce the original chaos carrier in the receiver. The message can be recovered by subtracting the synchronized chaos carrier from the transmission signal. The quality of chaos synchronization strongly affects the degree of the recovered message signal.

Let us look at the procedure of the chaos communication in detail. The chaotic system in the transmitter produces a chaotic carrier to mask the message signal. The encoded signal is sent to the receiver and it is used for both decoding the message and achieving synchronization of chaos. In the receiver, a similar chaotic system can reproduce a nearly identical chaotic carrier by adjusting with a set of the static parameter values that are considered as static keys to be shared beforehand. If the receiver succeeds in synchronizing chaos by using the chaotic hardware and the static keys, it can reproduce a similar chaotic carrier and can succeed in decoding the original message. The main purpose of chaos

communication is to hide the (existence) of a message by a chaotic carrier waveform, which is known as steganography, compared with the technique of hiding the (meaning) of the message, known as cryptography. One of the most important techniques in chaos communication is to share the same chaotic carrier between the distant users by using synchronization of chaos. To achieve synchronization of chaos, similar hardware systems as well as similar parameter values are required in the transmitter and the receiver. The tolerance of synchronization against parameter mismatch is one of the measures for the level of privacy in chaos communication, that is, narrow parameter regions for achieving synchronization result in more privacy since it is difficult for eavesdroppers to achieve synchronization of chaos. Recent advances on practical implementation of optical chaos communications will be described, including the demonstration of chaos communication in commercial optical-fiber networks at 2.5-10 Gb /s over a 100-km distance with low BER (Uchida, A., 2012). Several advanced techniques including photonic integrated circuits and forward error correction have been implemented in chaos communications. For chaos communications, it is necessary for two legitimate users to share a common secret key prior to the communication process. The system parameters provide a private key because the two communicating lasers must have nearly identical parameters, otherwise synchronization is failed. The distribution of a private key is the main weakness of any secure communication system, which is known as a secure key distribution problem (Uchida, A., 2012). Chaotic lasers could be useful for the physical implementation of secure key distribution based on information theory. The architecture based on chaotic lasers offers large key-establishing rates at long communication ranges. In

addition, optical transmitters and receivers used for conventional optical communication systems, including erbium-doped fiber amplifiers (EDFAs) and dispersion compensation fibers (DCFs), can be used for chaos-based secure key distribution without using specially designed hardware. Several schemes for chaos-based secure key distribution systems have been proposed and demonstrated as a new way of secure key distribution.

2.6.5 Random Number Generation with Chaotic Lasers

Another promising application with chaotic lasers is random number generation. The output of chaotic lasers provides fast temporal dynamics of Chaos with large spectral bandwidth. Typical bandwidth of semiconductor lasers is a few GHz, which is determined by the relaxation oscillation frequency. The speed of lasers is advantageous for the applications of physical random number generation. The combination of the characteristics of the complexity in chaos and large bandwidth in lasers could open up a new research field of fast physical random number generation. The output of chaotic devices could be both unpredictable as well as statistically random because they generate large-amplitude random signals from microscopic noise by nonlinear amplification and mixing mechanisms. The concept of random number generation is shown in a chaotic signal of laser output is detected by a photo detector and converted to a binary digital signal by an analog-to-digital converter (ADC). The ADC converts the input analog signal into a binary digital signal by comparing with the threshold voltage. The output binary random signal is a stream of bits. Random number generation with chaotic lasers has been intensively investigated since the first demonstration was published in 2008 (Uchida et al., 2008a). Many schemes have been

demonstrated and random-bit generation rates from 1.7 to 400 GB/s have been reported with verified randomness.

2.6.6 Controlling Chaos and Other Applications

Another direction of the research with chaotic lasers is controlling chaos, which is a natural way for engineering applications. Chaos needs to be avoided in many engineering systems, and the research on control and stabilization of chaos has strong motivation in nonlinear dynamical systems that are used for engineering applications. The research field on controlling chaos grew rapidly during the 1990s, where a chaotic temporal signal can be stabilized onto an unstable periodic orbit in a chaotic attractor based on control theory (Uchida, A., 2012). The aim of chaos control is to obtain a stable or periodic temporal waveform by adding a small external perturbation. The techniques for controlling chaos have been applied to many interdisciplinary research fields, because there have been many dynamical systems that are required to stabilize chaotic instabilities and fluctuations.

Other promising applications with chaotic lasers have been proposed. Remote sensing applications with chaotic lasers have been reported as chaotic lidar and radar systems. Blind signal separation using independent component analysis has been applied to chaotic temporal waveforms of laser output for the purpose of multiplexing communications. In addition, fractal optics have been used for wireless optical communication applications as a chaos mirror. Three research directions for engineering applications with chaotic lasers.

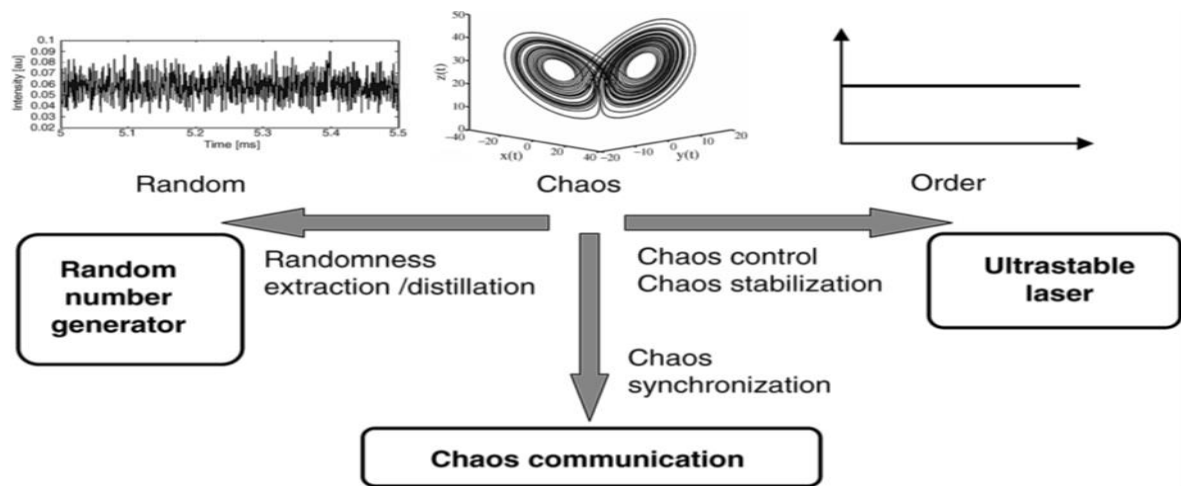


Figure 2.4. Three research directions for engineering applications with chaotic lasers.

The research directions with chaotic lasers for engineering applications are summarized in Figure 2.4. There are three main research directions treated in this book, related to the concepts of how to harness chaos. For chaos communication applications, the characteristics of chaos are used in a straightforward way, that is, the determinism of chaos results in synchronization ability of chaos, and the middle degrees of complexity are suitable to hide a message signal. By contrast, for the applications of random number generation, the randomness of chaos needs to be maximized and determinism of chaos needs to be eliminated by converting analog chaos signals to binary signals. The important technique is how to extract and distill the randomness from deterministic chaos for this application. The research on random number generation requires a new engineering approach of chaos for maximizing the randomness of chaos. By contrast, control and stabilization of chaos is a technique to completely avoid complexity and instability of chaos. To design and establish ultrastable lasers, chaos control techniques may be useful for the suppression of chaotic instabilities. The features of deterministic chaos including unstable periodic orbits can be utilized for controlling chaos. The

research on controlling chaos is the opposite direction of the research on random number generation, depending on minimizing or maximizing the complexity of chaos, respectively.

2.7 cross-Spectra and Coherence function

Coherence is a measure of the degree of relationship, as a function of frequency, between two time series, X_m and X_s . The concept can be motivated in many of ways. Power spectral density is the Fourier transform of correlation. From the discrete correlation theorem, we know that the Fourier transform of the correlation of two signals is equal to the product of a Fourier transform of one signal and a conjugated Fourier transform of the other. Therefore, power spectral density can be calculated with a Fourier transform. Additionally, the cross power density of two signals, x and y , can be computed as follows:

$$P_{xy} = Y X^* \quad (2.12a)$$

$$P_{xx} = X X^* \quad (2.12b)$$

$$P_{yy} = Y Y^* \quad (2.12c)$$

Can summarize in the form:

$$C_{xy} = \frac{|p_{xy}(f)|^2}{p_{xx}(f)p_{yy}(f)} \quad (2.13)$$

Where P_{xy} is the cross power spectral density of the two signals, x and y , while P_{xx} and P_{yy} are the power spectral densities of x and y respectively. Coherence is a function of frequency that measures the degree of linear dependency of two signals by testing whether they contain similar frequency components. The magnitude of coherence ranges from zero to one. At a given frequency, if the coherence is equal to (1) the two signals are considered to correspond to each other perfectly at that frequency. Conversely, a coherence which is equal to (0)

suggests that the signals are totally unrelated at that frequency. For computation, the signal is broken down into several sections for frequency component analysis using FFT. Adjacent sections can overlap, which helps to detect shared frequencies across sections. The size of FFT sections, window type and size, and the number of overlapping data points can affect the result. These choices should be made according to the nature of the input signals.

Chapter Three

Dynamical model theory

3.1 Introduction

The study of chaos in optical systems has been motivated both by the fundamental interest in dynamical systems theory as well as by practical applications (e.g., chaotic communications, and optimization of light collection systems). Optoelectronic semiconductor devices and, in particular, LD are ideal candidates for this kind of investigation. The chaotic spiking regime can be understood in terms of excitability of chaotic attractor. The excitable behavior is observed also on each of the periodic attractors within the period doubling cascade leading to chaos. The aim of study is demonstrate and explain theoretical model on chaotic spiking and excitability in semiconductor laser with optoelectronic feedback.

3.2 Chaotic spiking scenarios in DL with AM optoelectronic feedback

In this section we will study numerically the existence of chaotic spiking Sequences in the dynamics of a semiconductor laser with ac-coupled optoelectronic feedback, and illustrating the basic concepts of the theoretical model. The solitary laser dynamics is controlled by two coupled variables (intensity and population inversion) evolving with two very different characteristic timescales. The introduction of a third degree of freedom (and a third timescale) describing the ac-feedback loop, leads to a three-dimensional slow-fast system displaying a transition from a stable steady state to periodic spiking sequences as the dc-pumping current is varied. For intermediate values

of the current, a regime is found where regular large pulses are separated by fluctuating time intervals in a scenario resembling Homoclinic chaos (HC) (Al-Naimee, K., et al (2009)).

3.3 Dynamical model of chaos generation

The intra-band relaxation within the medium of the SL is fast enough of the order of (10^{-13}) s compared with the carrier recombination rate of (10^{-9}) s. This fact makes it possible to use approximately the model of two-level atoms for the theoretical investigation of the dynamics of semiconductor lasers (Ohtsubo, J., (2008) the approximate model of laser oscillations based on two-level atoms. While the population inversion in general laser systems is simply replaced by the carrier density produced by electron-hole recombination. The photon number (which is equivalent to the absolute square of the field amplitude) and the carrier density are frequently used as the variables of the rate equations for SLs. However, for the general descriptions of the dynamics in SLs, we must employ the complex amplitude of the field (the amplitude and the phase of the field) instead of the photon number. The field equation is a function of the time dependent carrier density and it is written as (Ohtsubo,J.,(2008)and Rogister, F.,et al (2001).

$$\frac{dE(t)}{dt} = \frac{1}{2} [(1 - i\alpha)g_n(N_t - N_{th})]E_t + E_{sp(t)} \quad (3.1)$$

where α parameter or line width enhancement factor, g_n the differential gain, N_t the carrier density at transparency, N_{th} the carrier density at threshold, and $E_{sp(t)}$ is the stochastic function corresponding to the zero-mean random field for spontaneous emissions, the field has the relation of

$$E_{sp(t)}E^*(t) = \frac{R_{sp}}{2} \quad (3.2)$$

The term R_{sp} is usually used for the effect of spontaneous emission in the photon number equation and is given by.

$$R_{sp} = \frac{\beta_{sp} \eta_{sp} N_t}{t_s} \quad (3.3)$$

Where β_{sp} is the coefficient of spontaneous emissions, η_{sp} is the internal quantum efficiency for spontaneous emissions, and t_s is the carrier lifetime in the laser cavity. We frequently omitted the term unless necessary since it is usually as small as $\beta_{sp} \approx (10^{-5})$. Furthermore, the investigation the fundamental dynamics of instability and chaos in nonlinear systems could be treated with only the deterministic terms without considering statistical noises. Noise is essentially considered as a separate effect from chaotic oscillations in as far as it is small. Using the notation of the complex field (Ohtsubo, J.,(2008) and Rogister, F., et al (2001).

$$E(t) = A(t) \exp(-i\varphi(t)) \quad (3.4)$$

The amplitude $A(t)$ and the phase $\varphi(t)$ of the field equation are separately given by.

$$\frac{dA(t)}{dt} = \frac{1}{2} g_n (N_t - N_{th}) A(t) \quad (3.5)$$

$$\frac{d\varphi(t)}{dt} = \frac{1}{2} \alpha g_n (N_t - N_{th}) \quad (3.6)$$

From the physical model of two-level atoms in SLs, the differential equation for the carrier density N , which is equivalent to the population inversion in common, lasers is given by:

$$\frac{dN(t)}{dt} = \frac{J}{ed} - \frac{N(t)}{t_s} - g_n (N(t) - N_0) A^2(t) \quad (3.7)$$

Where (J) is the injection current density and (d) is the thickness of the active layer. The first term on the right side of the equation is the pumping by the injection current. The second term is the carrier recombination due to spontaneous emissions. The carrier lifetime have been treated as a constant coefficient with a good approximation. The third term represents the carrier Recombination induced by the laser emission. The photon number inside the laser cavity is derived by the internal optical energy U and defined by the following equations.

$$S = \frac{U}{\hbar\omega} = \frac{\epsilon_0\eta\eta_e}{2\hbar\omega \int_{cavity} d3r |E_{real}(r)|^2} \quad (3.8)$$

Where (η) is the refractive index for the mode, (r) is the three-dimensional coordinate, and (E_{real}) is the real optical field inside the cavity. Assuming that the field inside the laser cavity is constant over the coordinate at a fixed time, the relation of the photon number (photon density) (S) and the real optical field (E_{real}) is approximated by

$$S = |E|^2 = \epsilon_0\eta\eta_e 2\hbar\omega |E_{real}|^2 V \quad (3.7)$$

Where (V) is the volume of the active layer. When rewrite the field amplitude (A), it is given by

$$A = S^{\frac{1}{2}} = \left(\frac{\epsilon_0\eta\eta_e V}{2\hbar\omega |E_{real}|} \right)^{\frac{1}{2}} \quad (3.9)$$

By summarizing the rate equations for the field amplitude, the phase, and the carrier density as follows.

$$\dot{A} = \frac{1}{2} g_n (N_t - N_{th}) A(t) \quad (3.10a)$$

$$\dot{\phi} = \frac{1}{2} \alpha g_n (N_t - N_{th}) \quad (3.10b)$$

$$\dot{N} = \frac{J}{ed} - \frac{N(t)}{t_s} - g_n (N_t - N_0) A^2(t) \quad (3.10c)$$

Ignoring the noise, the phase of the optical field is determined by $N(t)$ and $|A(t)|^2$ and is not an independent dynamical variable, so chaotic oscillations cannot appear without a nontrivial feedback, cause chaos cannot occur in a system of two ordinary differential equations. The time delay adds, in principle, an infinite number of other degrees of freedom, though in practice the number of active degrees of freedom involved in the observable laser dynamics depends on the size of t_R compared to the intrinsic times scales in the laser operation. We are not concerned with the dynamics of the optical phase in this system as it is removed by the use of the photo detector in the optoelectronic circuit. The dynamics of the photon density S and carrier density N can be described by the usual single-mode SL rate equations appropriately modified in order to include the ac-coupled feedback loop.

$$\dot{S} = (g(N - N_t) - \gamma_0)S \quad (3.12a)$$

$$\dot{N} = \left(\frac{I_0 + f_F(I)}{eV} \right) - \gamma_c N - g(N - N_t)S \quad (3.12b)$$

$$\dot{I} = \gamma_f I - K\dot{S} \quad (3.12c)$$

Where I is the high-pass filtered feedback current (before the nonlinear amplifier), $f_F(I) \equiv \frac{AI}{I+S_0I}$ is the feedback amplifier function, I_0 is the bias current, e the electron charge, V is the active layer volume, g is the differential gain, N_t is the carrier density at transparency, γ_0 and γ_c are the photon damping and population relaxation rate, respectively, γ_f is the cutoff frequency of the high-pass filter and k is a coefficient proportional to the photo detector responsibility. Compared with optical feedback, optoelectronic feedback is reliable and robust because the system is insensitive to optical phase variations (Rogister et al (2001) and Tang, S. and Liu, J.M.,(2001) and Solorio, J.S., et

al,(2002), for this reason the phase dynamics of the optical field can be eliminated. A detailed physical model of the experimental system should include also a series of low-pass frequency filters arising from the limited bandwidth of the photo diode, the electrical connections to the laser, parasite capacitances, and other undesirable electronic effects. However, we will see that such additional filters do not play a critical role in a qualitative description of the observed dynamics, which is the aim of the present model. For numerical and analytical purposes, it is useful to rewrite equations (3.12a), (3.12b), (3.12c), in dimensionless form. To this end, we introduce the new variables

$$x = \frac{gS}{\gamma_c} \quad (3.13a)$$

$$y = g\gamma_0(N - N_t) \quad (3.1b)$$

$$z = \left(\frac{gk}{\gamma_c} - x \right) \quad (3.13c)$$

And the time scale

$$t_0 = \gamma_0 t \quad (3.14)$$

The rate equations then become as follow:

Frist rate equation:

$$\dot{S} = (g(N - N_t) - \gamma_0)S$$

By substituting the following equations:

$$x = \frac{gS}{\gamma_c} \quad (3.16a)$$

by substituting the following equations:

$$S = \frac{x\gamma_c}{g} \quad (3.16b)$$

$$N - N_t = \frac{y\gamma_0}{g} \quad (3.16c)$$

$$\dot{t} = \gamma_0 t \quad (3.16d)$$

$$\frac{1}{dt} = \frac{\gamma_0}{dt} \quad (3.16e)$$

In equation (3.15).The first rate equations then become.

$$\dot{x} = x(y - 1) \quad (3.17)$$

The second rate equation.

$$\dot{N} = \left(\frac{I_0 + f_F(I)}{ev} \right) - \gamma_c N - g(N - N_t)S \quad (3.18)$$

By substituting the following equations in equation (3.18)

$$N = \frac{y\gamma_0}{g} + N_t \quad (3.19a)$$

$$f_F(I) = \frac{AI}{1 + SI} \quad (3.19b)$$

$$\alpha = \frac{Ak}{eV\gamma_0} \quad (3.19c)$$

$$A = \frac{e\alpha V\gamma_0}{k} \quad (3.19d)$$

$$\gamma = \frac{\gamma_c}{\gamma_0} \quad (3.19e)$$

$$z = \frac{gI}{k\gamma_c} - x \quad (3.19f)$$

$$gI = k\gamma_c(z + x) \quad (3.19g)$$

$$\dot{S} = \frac{Sg}{k\gamma_c} \quad (3.19h)$$

$$f(z + x) = \frac{\alpha(z + x)}{1 + S(z + x)} \quad (3.19i)$$

$$\dot{y} = \frac{g\gamma(I_0 - ev\gamma_c N_t)}{\gamma_0\gamma_c ev} + f(z + x) - y - xy \quad (3.19j)$$

$$I_{th} = ev\gamma_c \left(\frac{\gamma_0}{g} + N_t \right) \quad (3.19k)$$

$$\delta = \frac{I_0 - I_t}{I_{th} - I_t} \quad (3.19l)$$

Then the second rate equations become:

$$\dot{y} = \gamma(\delta - y + f(z + x) - xy) \quad (3.20)$$

The third rate equation can be modified by the following equation:

$$\dot{I} = -\gamma f I + k \dot{S} \quad (3.21a)$$

$$I = \frac{k\gamma_c(z+x)}{g} \quad (3.21b)$$

$$\frac{d}{dt} \left(\frac{k\gamma_c(z+x)}{g} \right) = -\gamma f I + k \dot{S} \quad (3.21c)$$

$$\frac{k\gamma_c\gamma_0(\dot{z} + \dot{x})(t)}{g} = -\gamma f I + k \dot{S} \quad (3.21d)$$

$$\dot{S} = \frac{\gamma_c\gamma_0 x(y-1)}{g} \quad (3.21e)$$

$$\dot{z} + \dot{x} = \frac{-\gamma f(z+x)}{\gamma_0} + x(y-1) \quad (3.21f)$$

$$\dot{z} = \frac{-\gamma f(z+x)}{\gamma_0} + x(y-1) - \dot{x} \quad (3.21g)$$

$$\dot{x} = x(y-1) \quad (3.21h)$$

$$\dot{z} = \frac{\gamma f(z+x)}{\gamma_0} \quad (3.21i)$$

$$\epsilon = \frac{\gamma_f}{\gamma_0} \quad (3.21j)$$

To

$$\dot{z} = -\epsilon(z+x) \quad (3.22)$$

The new rate equations after modification are:

$$\dot{x} = x(y-1) \quad (3.23a)$$

$$\dot{y} = \gamma(\delta - y + f(z+x) - xy) \quad (3.23b)$$

$$\dot{z} = -\epsilon(z+x) \quad (3.23c)$$

Where $f(z+x) \equiv \alpha \frac{z+x}{1+s(z+x)}$, $\delta_0 = \frac{I_0 - I_t}{I_{th} - I_t}$,

$I_{th} = \frac{ev}{\gamma_c} \left(\frac{\gamma_0}{g} + N_t \right)$ (is the solitary laser threshold current),

$\gamma = \gamma_c/\gamma_0$, $\alpha = Ak/ev\gamma_0$ and $S = \gamma_c \dot{S}k/g$

3.4 Amplitude modulation in Diode laser

3.4.1 Modulation

Modulation is the addition of information to an electronic or optical carrier signal. A carrier signal is one with a steady waveform, constant height (amplitude) and frequency. Information can be added to the carrier by varying its amplitude, frequency, phase, polarization (for optical signals), and even quantum level phenomena like spin. Common modulation methods include the following: Amplitude modulation (AM), in which the height (i.e., the strength or intensity) of the signal carrier is varied to represent the data being added to the signal. Frequency modulation (FM), in which the frequency of the carrier waveform is varied to reflect the frequency of the data. Phase modulation (PM), in which the frequency of the carrier waveform is varied to reflect changes in the frequency of the data (similar but not the same as FM). Polarization modulation, in which the angle of rotation of an optical carrier signal is varied to reflect transmitted data. Pulse-code modulation, in which an analog signal is sampled to derive a data stream that is used to modulate a digital carrier signal. Radio and television broadcasts and satellite radio typically use AM or FM. Most two-way radios use FM, although some employ a mode known as single sideband (SSB). More complex forms of modulation include phase-shift keying (PSK) and Quadrature Amplitude Modulation (QAM).

3.4.2 Modified Rate Equation with AM in Diode laser:

Here we use Amplitude modulation; the schematic diagram of directly modulated semiconductor lasers with a delayed optoelectronic feedback is shown in Fig.3.1. The diode laser (DL) is produce light signal, this light signal output from the laser diode is converted into electronic signal using a photo

detector (PD) and then amplified to the required gain. Modulated factor $((1 + H) x)$ where (H) is modulation current depends on the modulation depth is fed back to the input of the laser diode in addition to its injection current. Allowing the light to travel a certain distance through free space before reaching the (PD) can provide the required delay. For GHz modulation, the delay is of the order of nanoseconds that correspond to a traveling distance of the order of a few centimeters. For a negative feedback it is deducted from the total input current comprising of the bias and modulation factor. Feedback control is more commonly used than open-loop or feed forward control. Then we can define the main characteristics of Closed-loop Control as being:

To reduce errors by automatically adjusting the systems input, to improve stability of an unstable system, to increase or reduce the systems sensitivity, to enhance robustness against external disturbances to the process and to produce a reliable and repeatable performance.

Correspondingly the equation for the input current will be modified as follows.

$$\dot{z} = -\epsilon(z + x) + (1 + H)\dot{x} \quad (3.24)$$

where H is sinusoidal current of modulation represent in the following equation:

$$H = A \sin(2\pi ft) \quad (3.25)$$

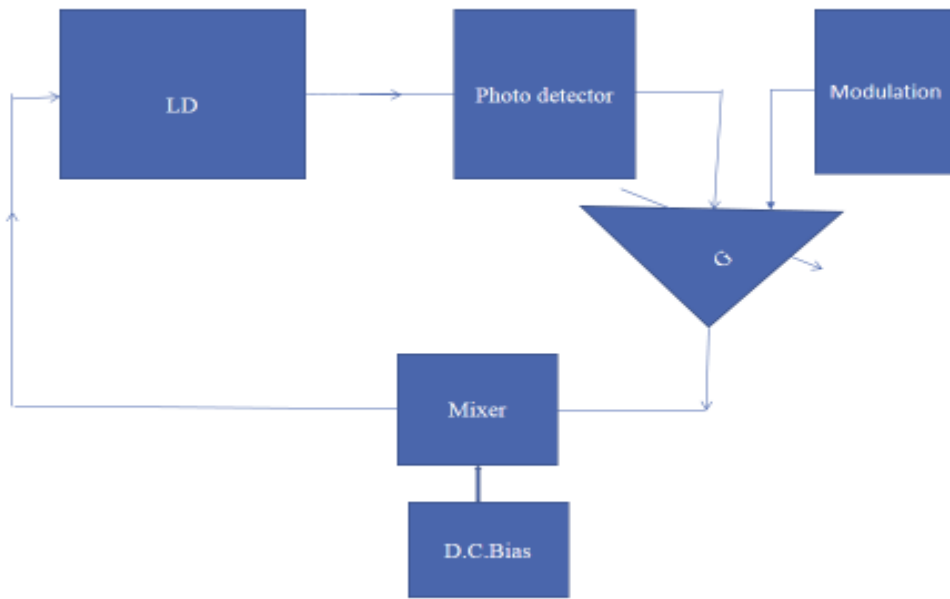
Here we examine the effect of the amplitude of the modulation term (A) on the dynamical system while the frequency is remain constant equal to $(f=1\text{GHz})$.

Three rate equations after our modification become:

$$\dot{x} = x(y - 1) \quad (3.26a)$$

$$\dot{y} = \gamma(\delta - y + f(z + x) - xy) \quad (3.26b)$$

$$\dot{z} = -\epsilon(z + x) + (1 + A\sin(2\pi ft))\dot{x} \quad (3.26c)$$



10 September 2017

17

Figure 3.1: Schematic diagram of directly modulated semiconductor lasers

3.5 Dynamical Model of Unidirectional Coupling Oscillators

We consider continuous wavelet transform to the two time series obtained from the two chaotic time-delayed systems, with small variation in initial condition. Fig.3.2 describes the identical synchronization configuration model. To investigate synchronization, we coupled two lasers Master and Slave by



Figure 3.2: Unidirectional coupling Sketch of two delayed laser.

By using modified equations (3.23) with modulation term for both (Master and Slave) we obtain. For the master:

$$\dot{x}_m = x_m(y_m - 1) \quad (3.26a)$$

$$\dot{y}_m = \gamma(\delta - y_m + f(z_m + x_m) - x_m y_m) \quad (3.26b)$$

$$\dot{z}_m = -\epsilon(z_m + x_m) - c x_m \quad (3.26c)$$

For the slave:

$$\dot{x}_s = x_s(y_s - 1) \quad (3.27a)$$

$$\dot{y}_s = \gamma(\delta - y_s + f(z_s + x_s) - x_s y_s) \quad (3.27b)$$

$$\dot{z}_s = -\epsilon(z_s + x_s) - c(x_s - x_m) \quad (3.27c)$$

In the present configuration the coupling factor was used as sinusoidal current equation depend on amplitude and frequency.

$$C = A \sin(2\pi f t) \quad (3.28)$$

Where (A, f) is the coupling factor amplitude and frequency, respectively, here was examined the effect of the variation in the amplitude of the added term while the frequency remain constant.

3.6 Dynamical Model of Bidirectional Coupling Oscillators

Here apply the synchronization conditions $\dot{x}_m - \dot{x}_s$ to the Master oscillator as modulation term in third equation rate and $\dot{x}_s - \dot{x}_m$ to the slave oscillator system, fig. (2.6) describe the schematic diagram. Then the consequences for chaos synchronization was discussed by (Ohtsubo, J., (2008).

By using modified equations (3.26) with coupling factor term for both (Master and Slave) we obtain. For the master:

$$\dot{x}_m = x_m(y_m - 1) \quad (3.29a)$$

$$\dot{y}_m = \gamma(\delta - y_m + f(z_m + x_m) - x_m y_m) \quad (3.29b)$$

$$\dot{z}_m = -\epsilon(z_m + x_m) - g(\dot{x}_m - \dot{x}_s) \quad (3.29c)$$

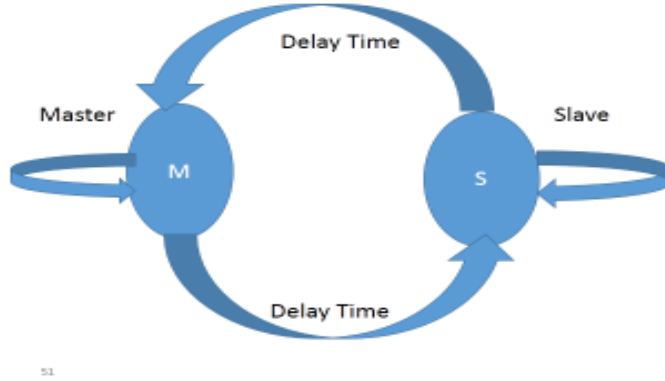


Figure 3.3: Bidirectional Sketch of two coupling delayed laser.

For the slave:

$$\dot{x}_s = x_s(y_s - 1) \quad (3.30a)$$

$$\dot{y}_s = \gamma(\delta - y_s + f(z_s + x_s) - x_s y_s) \quad (3.30b)$$

$$\dot{z}_s = -\epsilon(z_s + x_s) - g(\dot{x}_s - \dot{x}_m) \quad (3.30c)$$

$$g = A \sin(2\pi ft) \quad (3.31)$$

In the present configuration we recall coupling factor (g), here we examine the effect of the variation of the amplitude (A) of the coupling factor on the synchronization process while the frequency remain constant also.

Chapter Four

Results and Discussion

4.1 Introduction

In this study, the theoretical approach of modulated laser chaos by optoelectronic feedback in the laser diode is achieved. Effects of the amplitude modulation term have been illustrated. Berkeley Madonna and Origin software are used to analyze the time series generated in the chaos regime. The analysis concerns the study of the attractors and the Fourier transformations of the output spectrum. The results of numerical investigations on the effect of amplitude modulation on the dynamics of Diode lasers were illustrated. The study was undertaken to find out the possibility of obtaining chaotic outputs of Diode laser under small amplitude values. The nonlinear dynamics of semiconductor lasers with current modulation was investigated.

4.2 Effect of modified model with amplitude AM on chaos dynamic

In our suggested model the transition from a chaotic spiking to stationary steady state and eventually periodic self-oscillations as the amplitude of the modulation current was varied as explained in chapter three with Fig.(3.1), and the time series of the output that were registered for different values of the injected amplitude modulation. The modeling approach of this scenario was investigated by programming the physical model, where the total simulation time chosen depends strongly on the magnitude of the temporal scales defined by the parameters γ and ϵ , between the chaotic spiking and steady state (belonging to the initial value of the feedback strength), the system passes

through a cascade of period doubled and chaotic attractors of small amplitude. By using Berkeley Madonna software where the feedback strength ϵ is fixed to 2×10^{-5} , $\gamma = 1 \times 10^{-3}$, $\alpha = 1$, $S = 11$, $\delta = 1.01702$. While the initial conditions were: $x_m = 0.0219$, $y_m = 1$, $z_m = 0.005$. The bias current δ is constant in this case. The observed intensity spectra with the increase of the amplitude of the modulated current are shown in figures number (4.1, 4.2, 4.3, 4.4, 4.5), of the time series, corresponding FFT and attractors.

Figure (4.1a) shows some spikes with high amplitudes in dynamic time series, at the value of the Amplitude modulated current ($A = 0.060$) the chaotic state was appeared. In the corresponding attractor of chaotic behavior, the trajectories are different in diameters and dense fig.(4.1b). While the corresponding FFT of this state fig.(4.1c) shows the signature of chaotic behavior, where the distribution is decay exponentially. The (x) axis in the figures represents photon density and (y) axis represents carrier density.

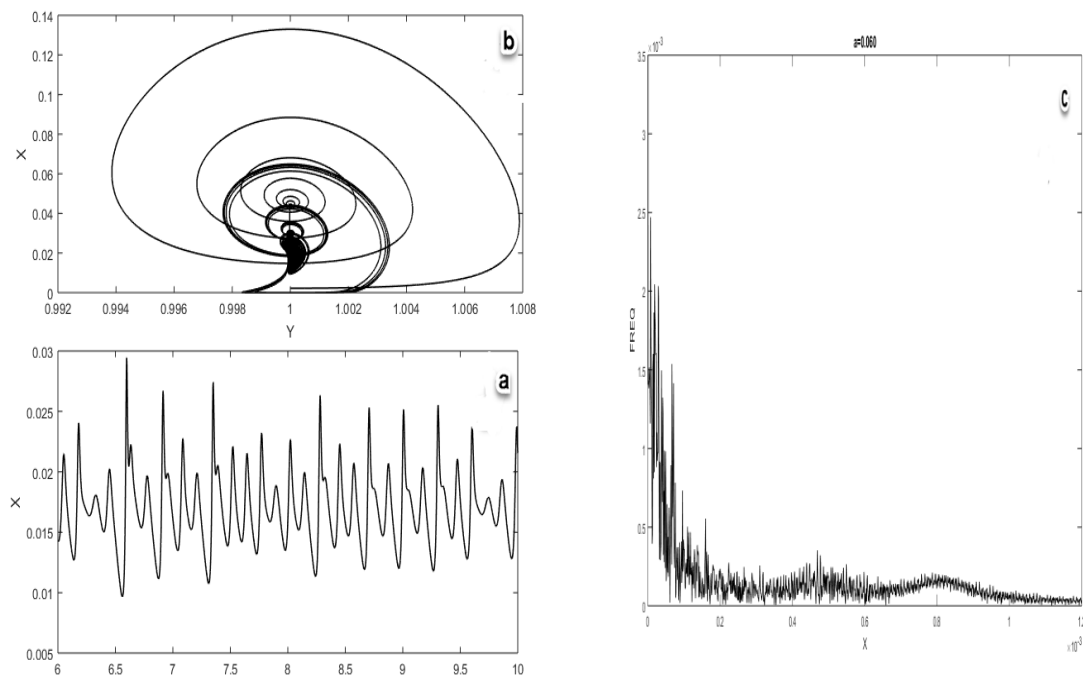


Figure 4.1: a) Time series of dynamical model b) Attractor and c) Fourier transform when ($A = 0.060$)

When (A) increased to (0.075), system converted to the period doubling state, with different frequency was appeared in fig. (4.1a) high and low intestines while (f) remain constant. The corresponding attractor is in figure (4.2b). The FFT diagram in figure (4.2c) has also different frequency.

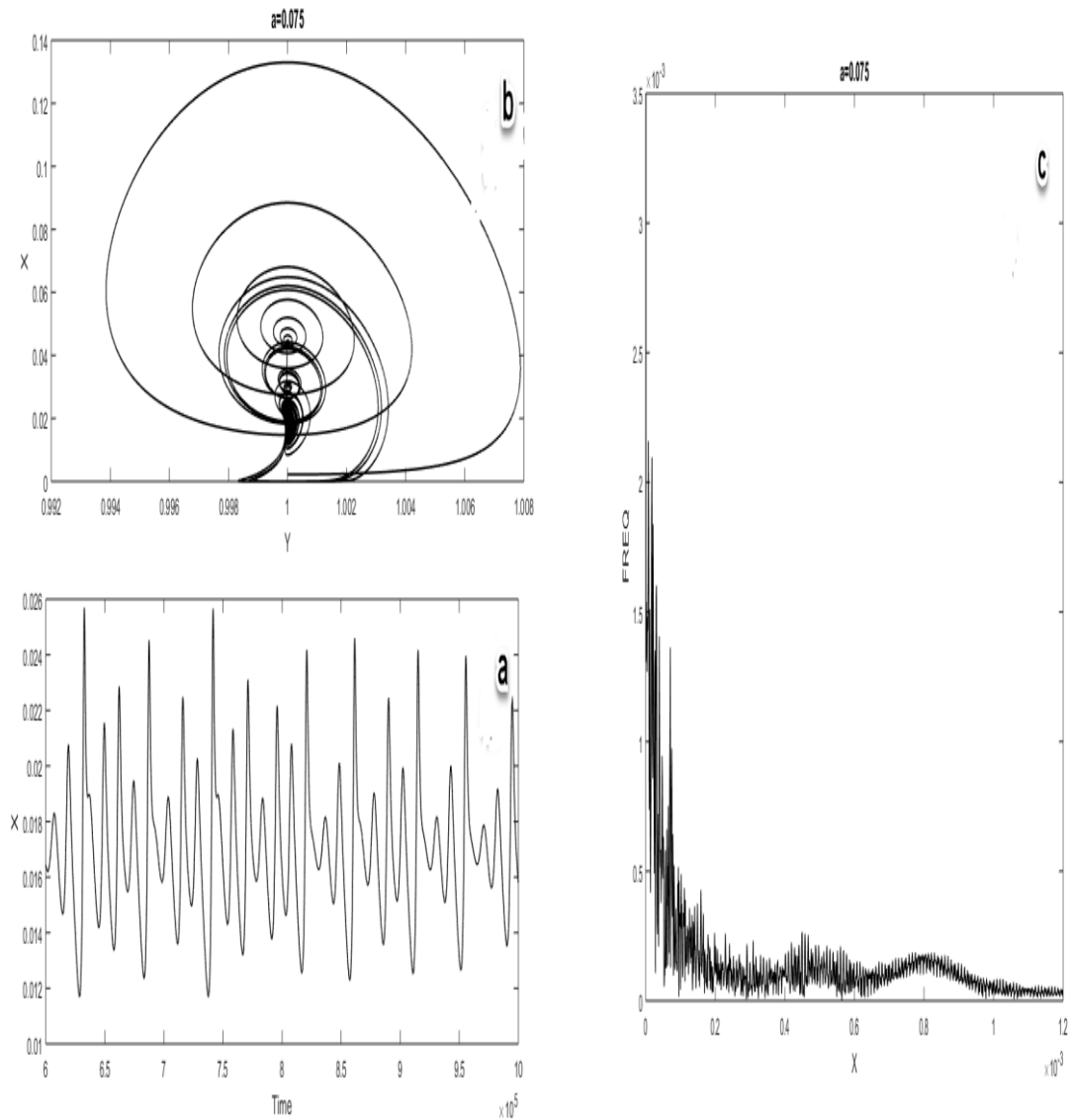
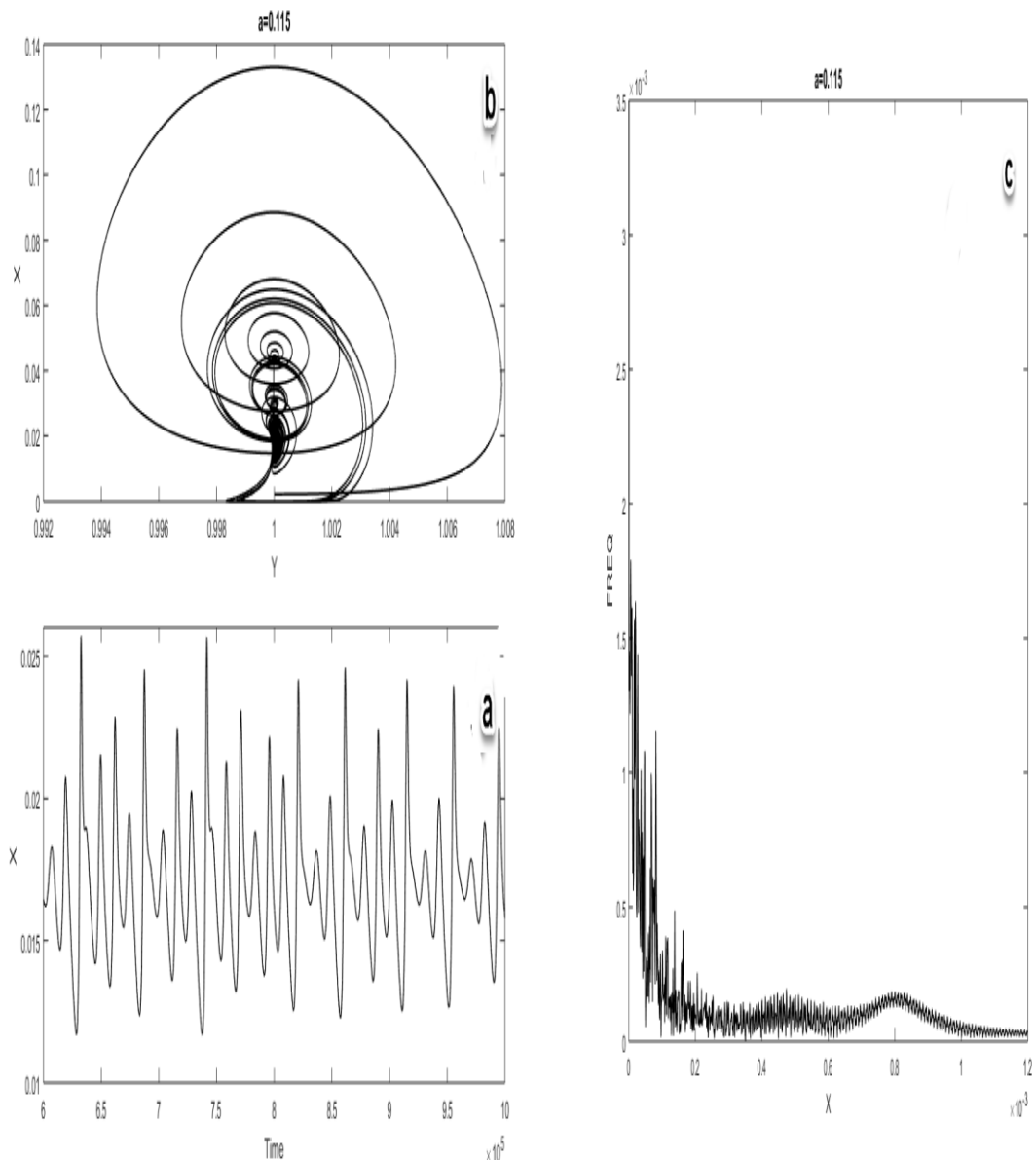


Figure 4.2: a) Time series of dynamical model b) Attractor and c) Fourier transform when (A=0.075)

In Fig. (4.3a) the period doubling state is remain while the amplitude increasing to the ($A=0.115$). The corresponding attractor of period doubling state is represented in Fig. (4.3b) is differ than other one in Fig. (4.2b) the small and large periods referring to the small and large peaks. Fig. (4.3c) shows the corresponding FFT of this state.



**Figure 4.3: a) Time series of dynamical model b) Attractor and c) Fourier transform
When ($A=0.115$)**

Fig. (4.4a) illustrated the transition from periodic doubling state to periodic state when the amplitude is increased into ($A = 0.199$), Fig. (4.4b) clarify the corresponding FFT of periodic state, seen that peaks in time series appear as a fixed frequencies. In the corresponding attractor of periodic state, the small peaks appears as a periodic orbits in Fig. (4.4c).

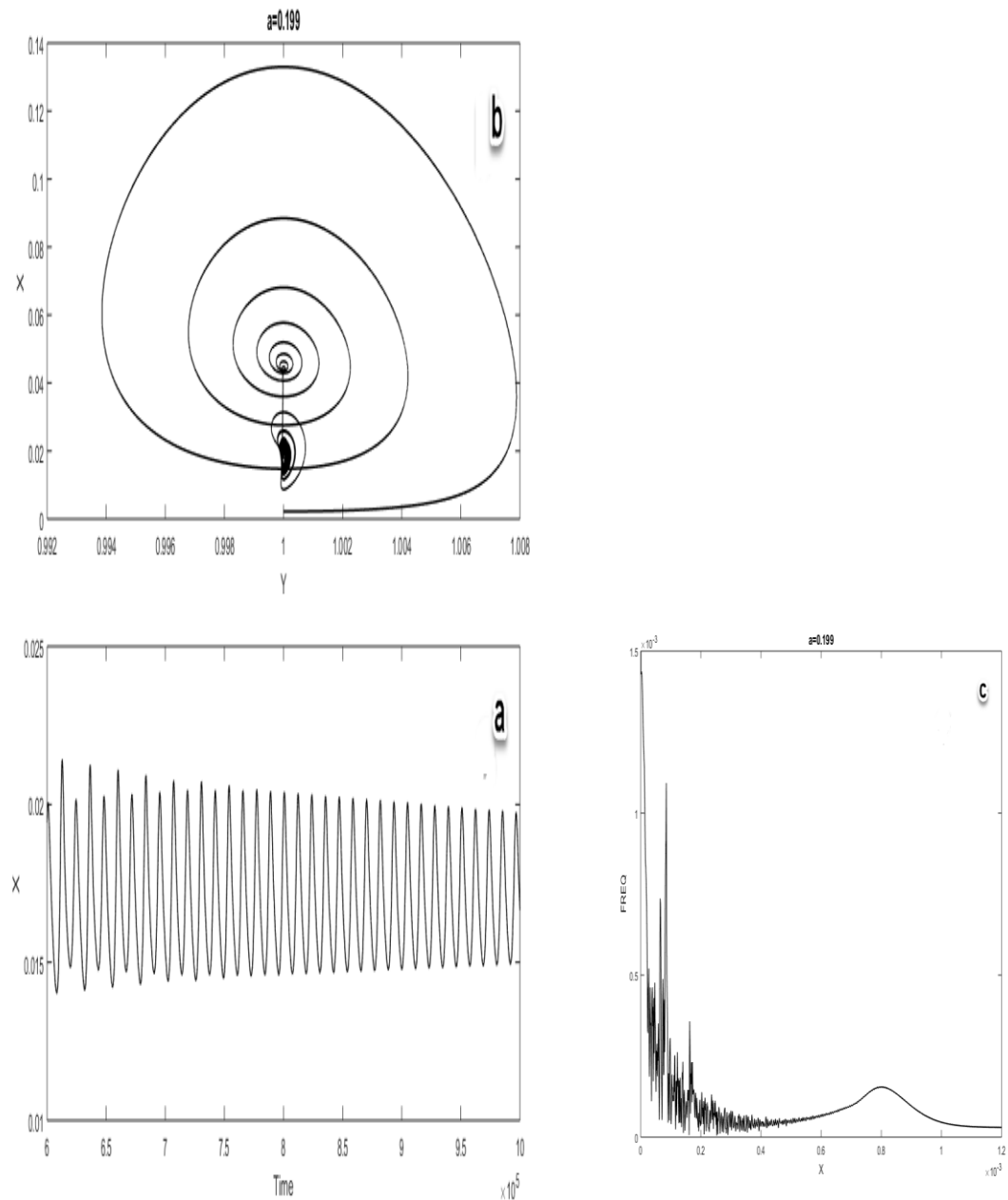


Figure 4.4: a) Time series of dynamical model b) Attractor and c) Fourier transform when ($A=0.199$)

Fig. (4.5a) shows the steady state, where the magnitude of the amplitude on the system ($A=0.656$) and modulation frequency ($f=1\text{GHz}$) while fig.(4.5b) represents the corresponding attractor for steady state as a spiral fixed point. Fig. (4.5c) represent Fourier transform of steady state.

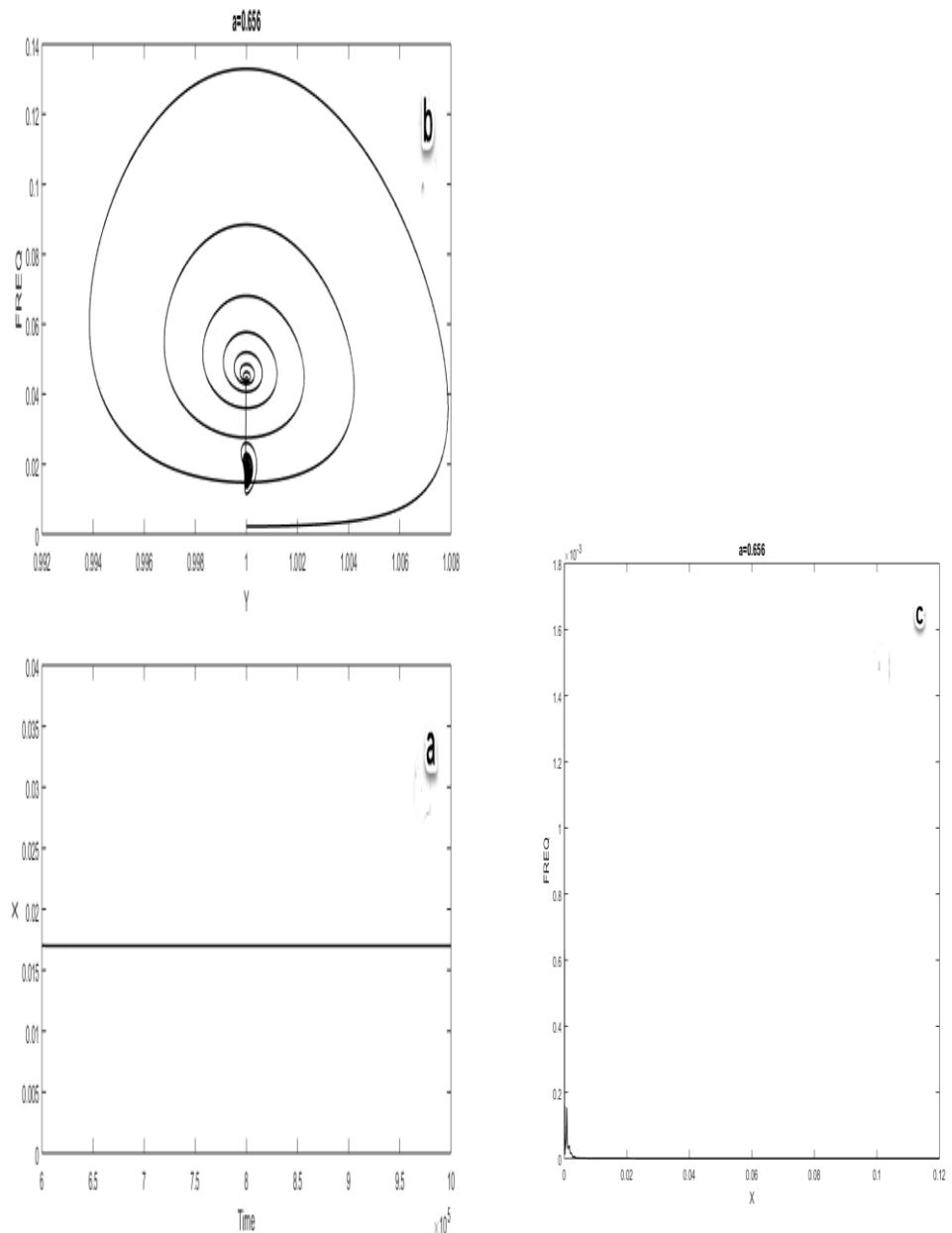


Figure 4.5: a) Time series of dynamical model b) Attractor and c) Fourier transform when ($A=0.656$)

Fig. (4.6a) shows chaotic state, where the magnitude of the amplitude on the system ($A=0.060$) and modulation frequency ($f=1\text{GHz}$) while the feedback strength change to ($\varepsilon = 3 \times 10^{-5}$). Fig.4.6b represents the corresponding attractor for chaotic state it's denser than fig.1. Fig. (4.6c) represent Fourier transform it's appear with several frequencies.

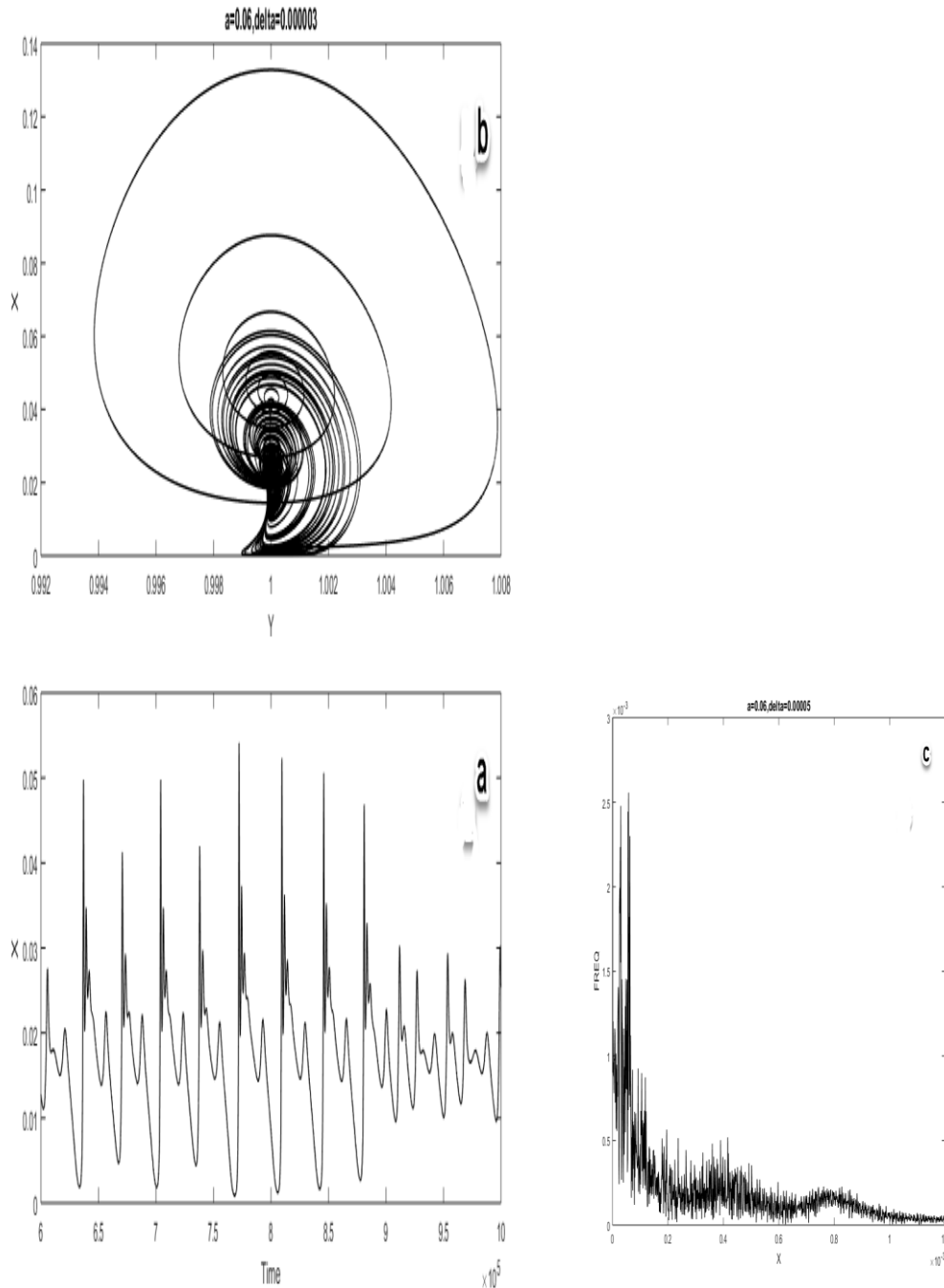


Figure 4.6: a) Time series of dynamical model b) Attractor and c) Fourier transform when ($A=0.060$)

The bifurcation diagram (Fig.4.7) is computed by varying (A) over a small interval contiguous to the initial Hopf bifurcation. As (A) approaches the turning point (when its value becomes greater than 0.081) the chaotic amplitude fluctuations are sufficiently low trigger fast dynamics. This results in an erratic-sensitive to initial condition-sequence of Homoclinic spikes on top of a chaotic background.

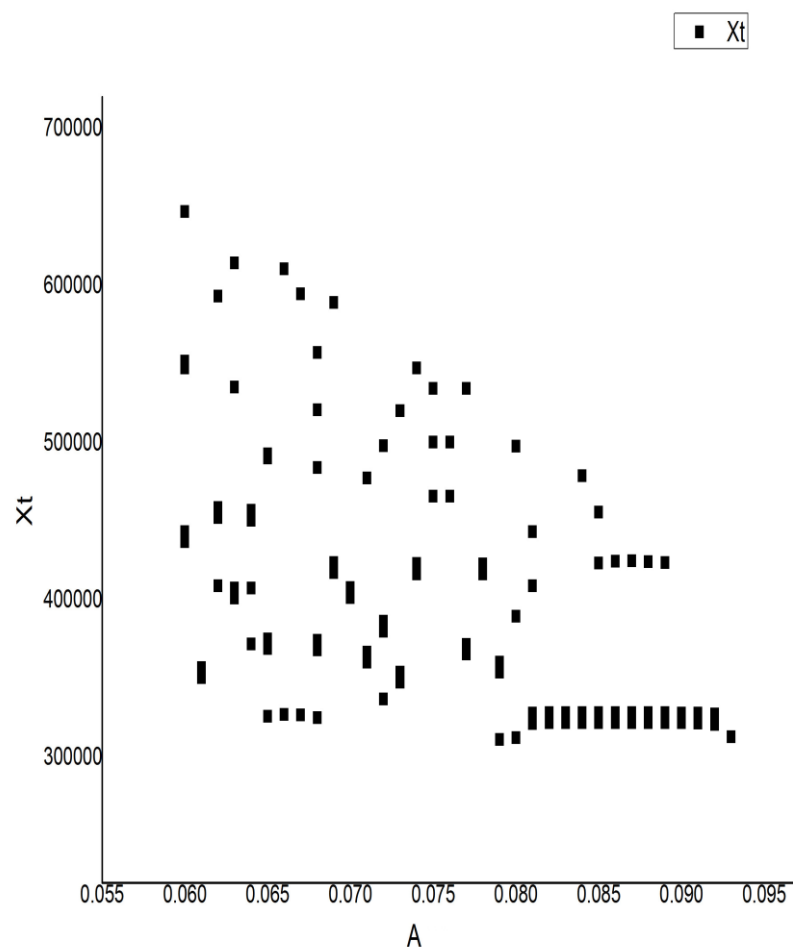


Figure 4.7: Bifurcation diagram for the model equations other parameters Constant

4.3 Effect of variation AM in unidirectional coupling

We start simulation when a and f are zero in the model and the initial state for Master-Slave is: $x_m=0.021$, $y_m=1$, $z_m=0.005$ and $x_s=0.022$, $y_s=1$, $z_s=0.005$.

$\epsilon = 2 \times 10^{-5}$, $\gamma = 1 \times 10^{-3}$, $\alpha = 1$, $s = 11$, $\delta = 1.01702$. To investigate the synchronization between two coupled lasers unidirectional we apply the condition of synchronization as we mentioned in the previous chapter

Section 5. Here we illustrate the results of numerical investigations on the effect of directly delayed modulated amplitude on the dynamics of master-slave lasers Diode unidirectional coupling. The study was undertaken to find out the possibility of synchronization step outputs under small values of amplitude while frequency was constant equal to ($f=4$). The synchronization of two semiconductor lasers with current modulation was investigated when ($a=0.4101$). The relation between coherence as function in the frequency was shown in full synchronization, partial synchronization and unsynchronized coupling also we show the relation between the coherence function and variation amplitude.

Fig.4.8A. show the coherence function between photon density output of the master and Slave y-axis and frequency in x-axis about ($c=0.75$) when the amplitude is ($a=0.4098$) and ($f=4$). Notching from the magnitude of the coherence function and dynamics time series of Master and Slave there are partial synchronization. Fig.4.8B reveals the dynamic of two oscillators.

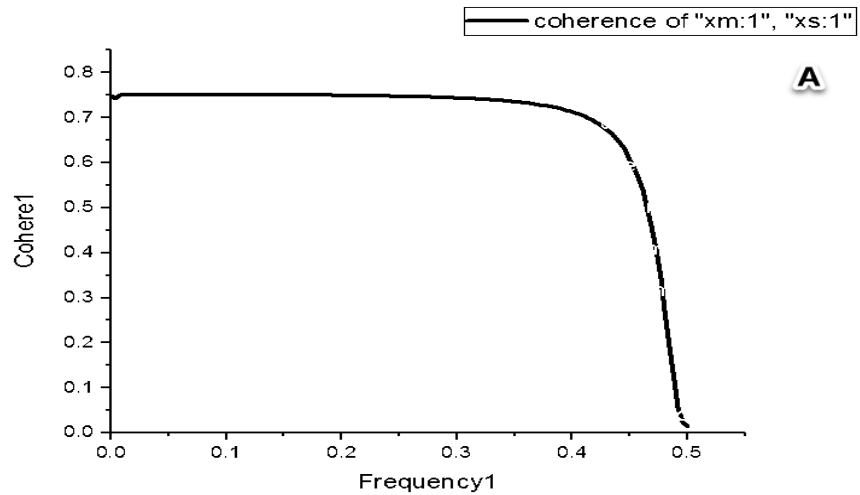


Figure 4.8a: coherence function when ($a=0.4098, f=4, c=0.74$)

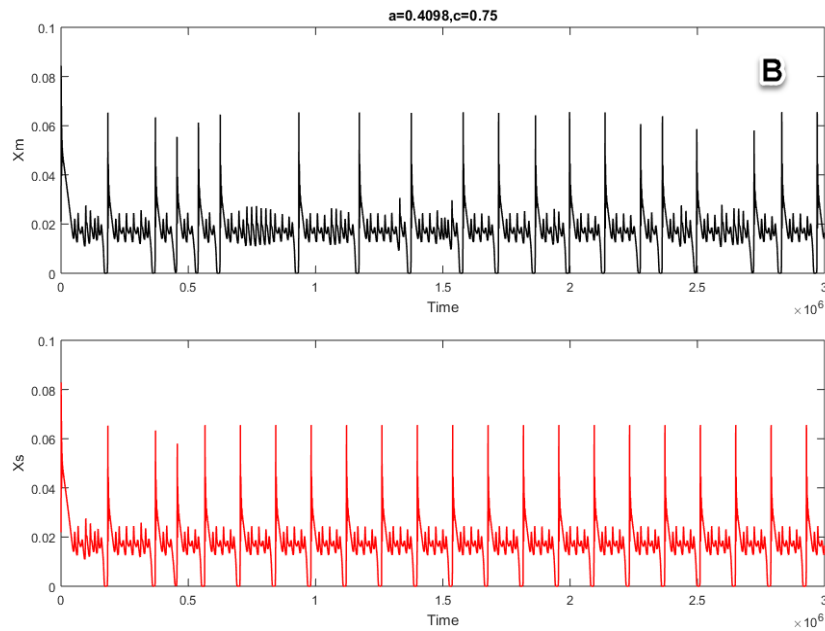


Figure 4.8b: Dynamical time series of two LD and coherence when ($a=0.4098, f=4$)

Fig.4.9A. illustrated the coherence function about ($C=0.98$) when the amplitude increase to ($a=0.4101$) with constant frequency. Showing the transition from partial synchronization step to full synchronization step and Fig.4.9B. Show the dynamic time series of two oscillators.

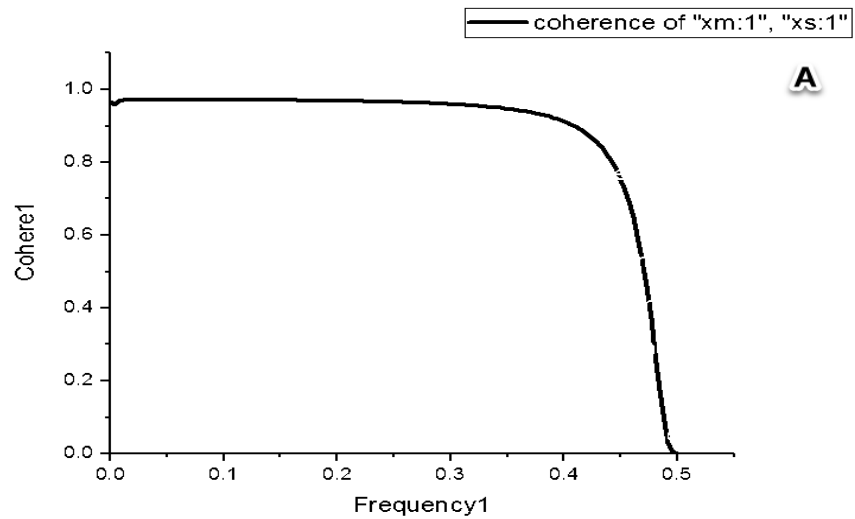


Figure 4.9a: coherence function when ($a=0.4101$, $c=0.98$)

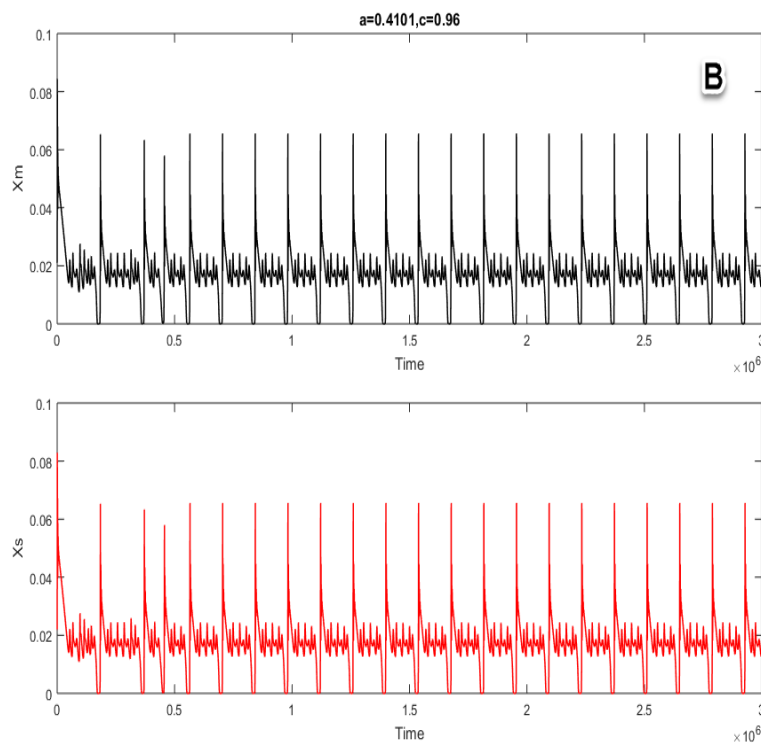


Figure 4.9b: Dynamical time series of two LD when ($a=0.4101$)

Fig.4.10A. clarify the coherence function between two oscillators when the frequency remain constant and the amplitude are ($a=0.4102$) noticing that from the magnitude of coherence function it is unsynchronized equal to ($C=0.71$) and Fig.4.10B. Show the dynamic time series of two oscillators.

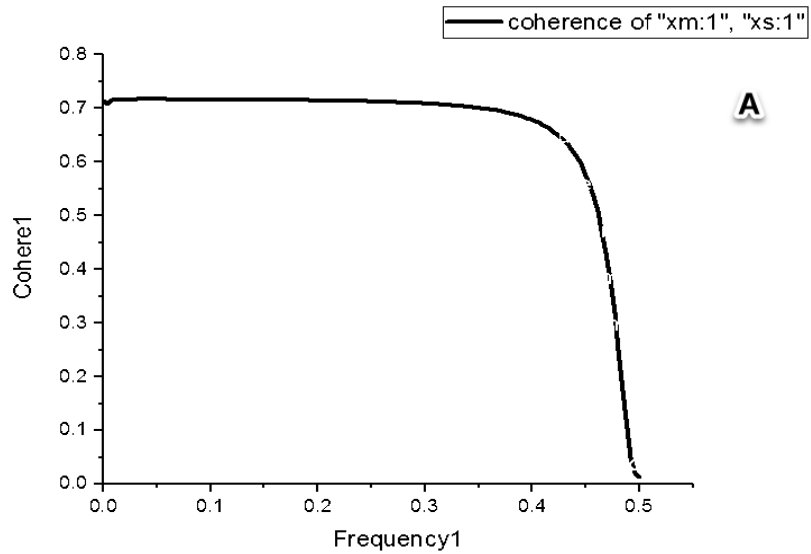


Figure 4.10a: coherence function when ($a=0.4012$, $c=0.71$)

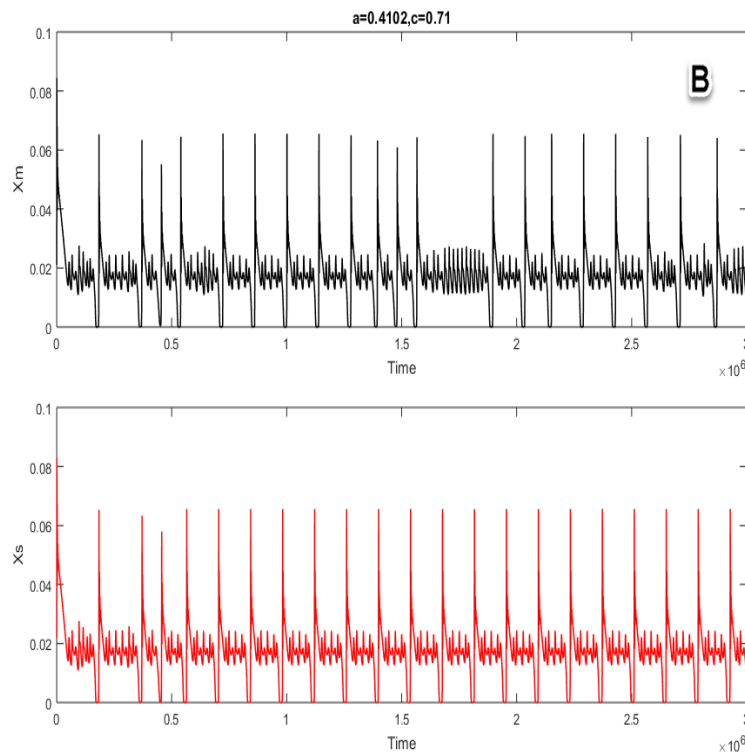


Figure 4.10b: Dynamical time series of two LD when ($a=0.4012$).

4.4 Effect of variation AM in bidirectional coupling

we start simulation when a and f are zero in the model and the initial state for Master-Slave is: $x_m=0.021, y_m=1, z_m=0.005$ and $x_s=0.022, y_s=1, z_s=0.005$ feedback strength ϵ is fixed to 2×10^{-5} , $\gamma = 1 \times 10^{-3}$, $\alpha = 1$, $s = 11$, $\delta_1 = \delta_2=1.01702$. To investigate the synchronization between two coupled lasers we apply the condition of synchronization as we mentioned in the previous chapter section 6. Here we illustrate the results of numerical investigations on the effect of directly delayed modulated amplitude on the dynamics of master-slave lasers Diode bidirectional coupling. The study was undertaken to find out the possibility of synchronization step outputs under small values of amplitude while frequency was constant equal to ($f = 4$). The synchronization of two semiconductor lasers with current modulation was investigated when ($a=1.55$).The relation between coherence as function in the frequency was shown in full synchronization, partial synchronization and unsynchronized coupling also we show the relation between the coherence function and variation amplitude.

Fig. (4.11A) represent coherence function ($C=0.96$) and Fig.4.11B. Represent time series of two coupled laser when ($a=1.56$) and frequency remain constant noticing here partial synchronization step.

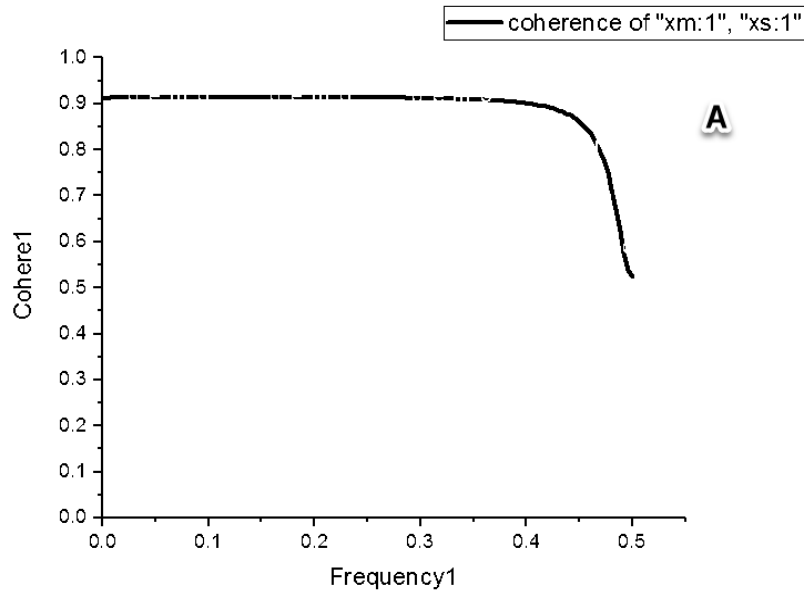


Figure 4.11a: coherence function when ($a=1.56, c=0.96$)

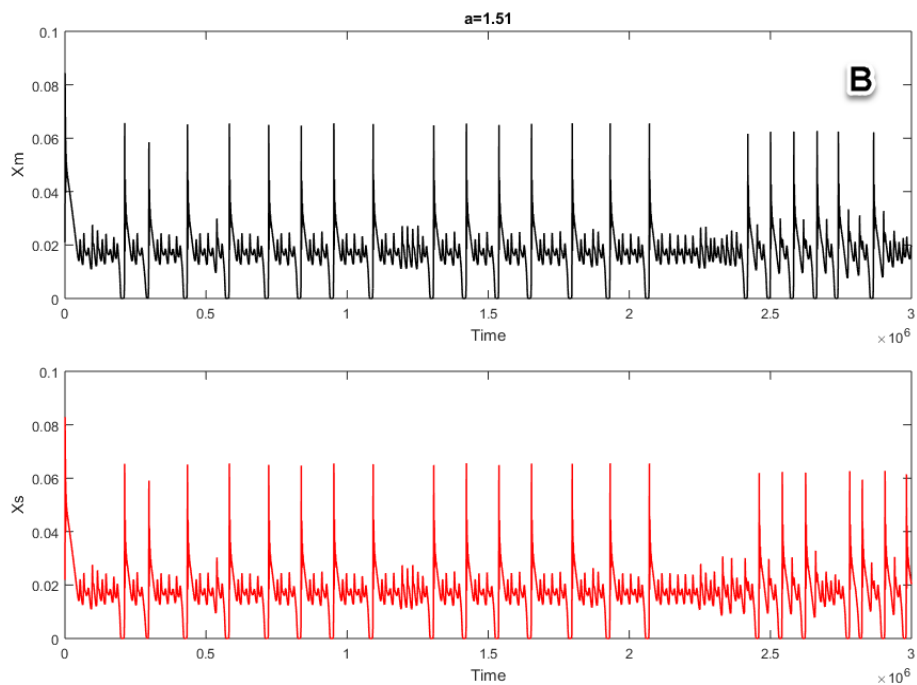


Figure 4.11b: Dynamical time series of two coupled laser and coherence function when ($a=1.56$)

Fig. (4.12A) illustrate Coherence function equal ($C=1$) and fig.4.12B show the time series of two coupled laser when ($a=1.55$). Noticing here the full synchronization step was appearing.

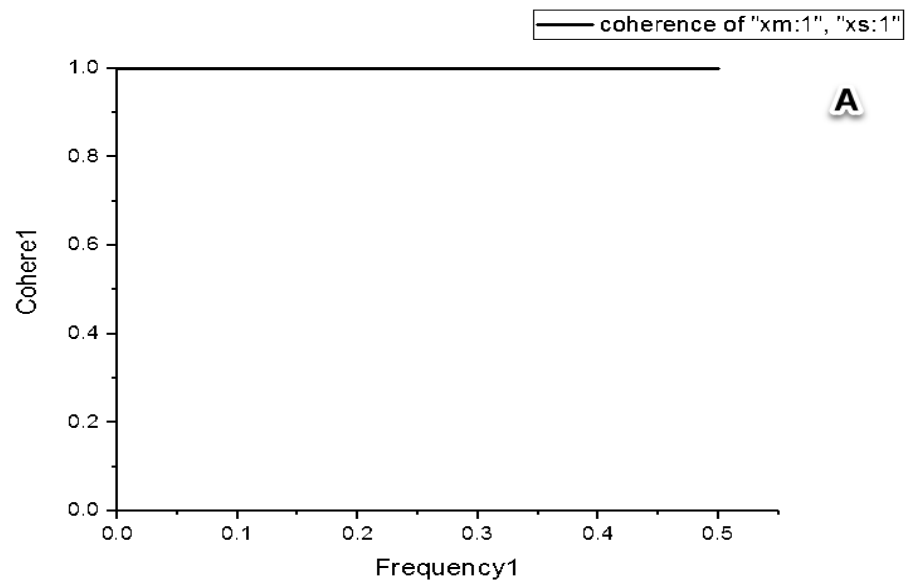


Figure 4.10: coherence function when ($a=1.55$)

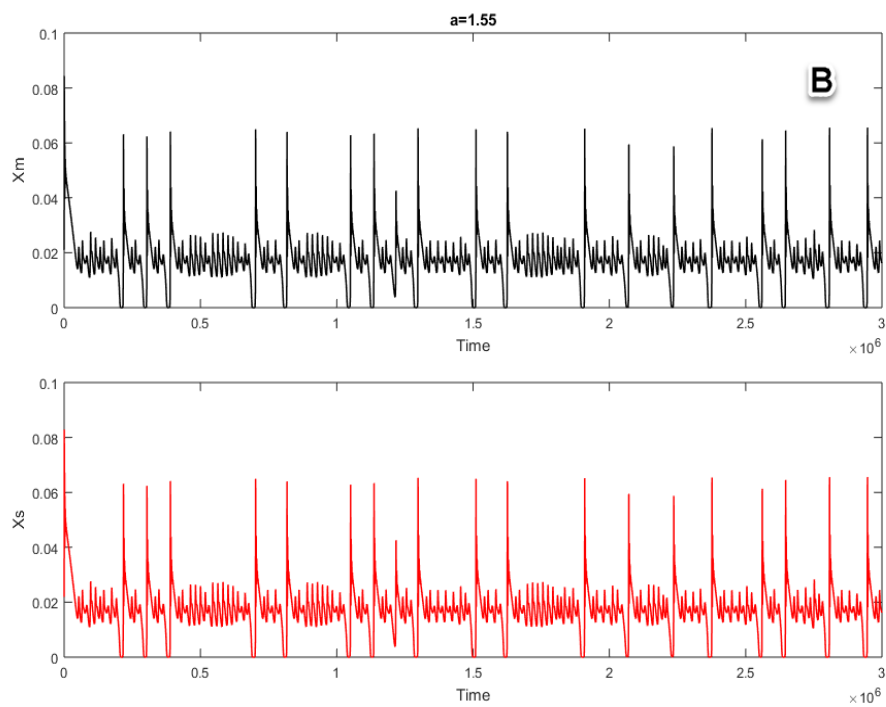


Figure 4.11: Dynamical time series of two coupled laser when ($a=1.55$)

Fig. (4.12B) avouch the unsynchronized step when the amplitude of coupling factor is ($a=1.50$) and the frequency was ($f = 4$). Fig.4.12A. show the coherence function about ($C=0.8$).

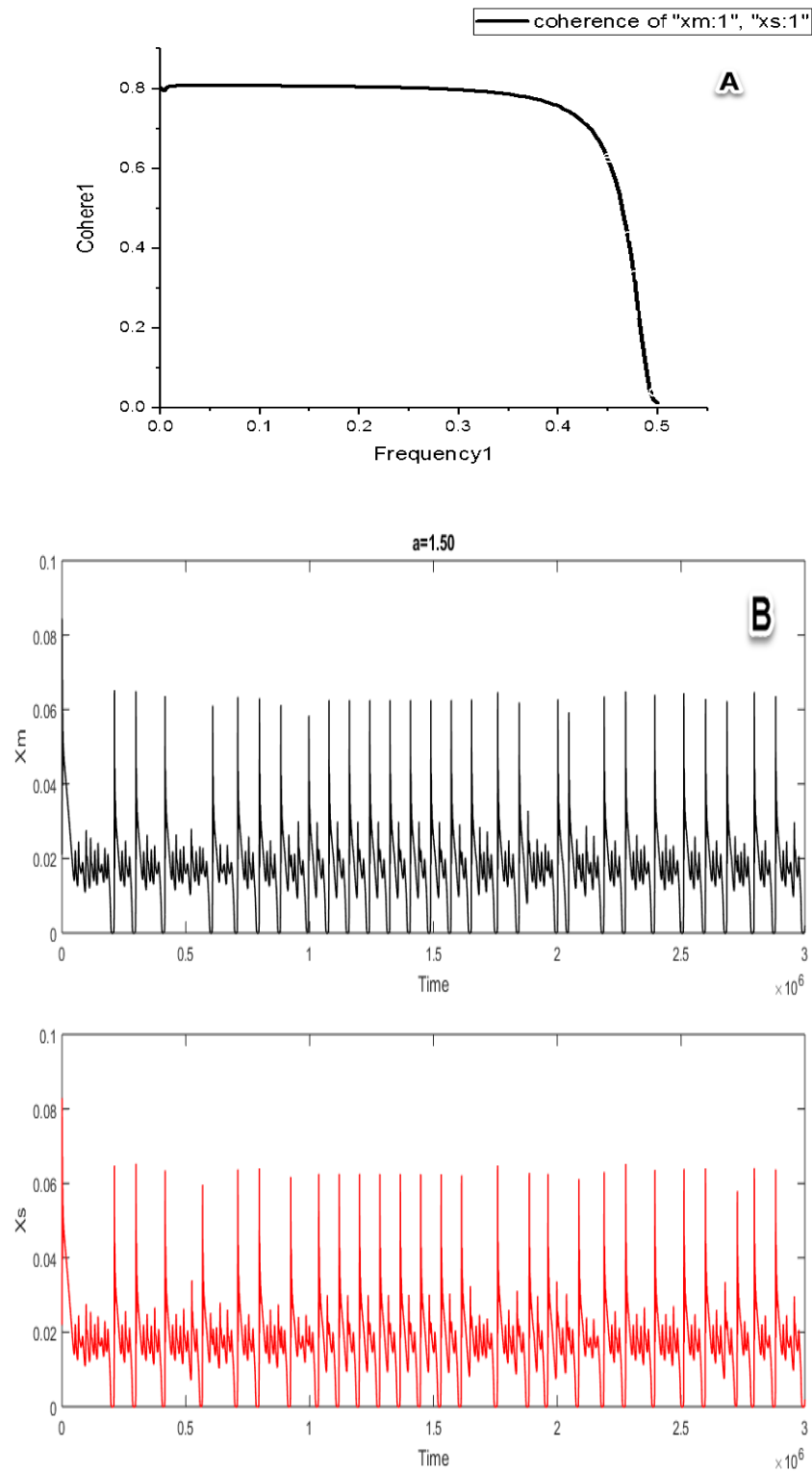


Figure 4.12: Dynamical time series of two coupled laser and coherence function when ($a=1.50$).

4.4 Dissections

When the Master and Slave are identical and coupled unidirectional, where the dynamical variables of both are equal in time is a solution for the coupled system. To determine the sensitivity of our setup to parameter mismatch in real Lasers, we evaluated a measure of synchronization. We found numerically, that for ($a=0.4101$), this solution is stable and synchronization of the electric field and the carrier density in Master and Slave is accomplished. And coherence function equal to ($C=0.98$ approach to 1) this refer to full synchronization we furthermore showed in the fig.4.9 it can be seen that after a short transient the two output signals become unsynchronized. The detuning between amplitude of the two lasers plays a crucial role for identical synchronization. Even a small amplitude detuning prevents the lasers from synchronizing, as seen in Fig.4.8. Partial synchronization. In this unidirectional coupling configuration, the coupling delay (ϵ) between the Master and the Slave, does not play any role in the synchronization process.

When the Master and Slave are identical and coupled bidirectional, all other control parameters in the system are constant.

For ($a=1.55$), this solution is stable and synchronization of the electric field and the carrier density in Master and Slave is investigated. And coherence function equal to ($C=1$) this refer to full synchronization we furthermore showed in the fig.4.10 it can be seen that after a short transient the two output signals become unsynchronized. Even a small amplitude detuning prevents the lasers from synchronizing, as seen in Fig.4.11. Partial synchronization.). We furthermore

showed in the fig.4.12 it can be seen the two output signals become unsynchronized. When ($a = 1.50$) and coherence function about ($C = 0.8$) in this bidirectional coupling configuration, the coupling delay (ε) between the Master and the Slave also, does not play any role in the synchronization process

4.5 Conclusion

A delayed optoelectronic feedback diode laser is employed to study the ability of obtaining chaotic output from a directly modulated semiconductor laser under GHz modulation frequency. The results showed the effect of small window modulation amplitude on the output dynamics in the range ($0.006 > a > 0.656$) when all other control parameters are kept constant at the chaotic operating condition. The transition from a chaotic spiking to stationary steady state and eventually periodic self-oscillations as the amplitude of the modulation current was varied as explained in chapter three also we demonstrate the instability of the system by bifurcation diagram so the modulation amplitude is sensitive in output dynamic. The optoelectronic delayed feedback laser diode can be controlled to get at a given nonlinear state, such as the single-periodic, periodic doubling, quasi chaotic, chaotic by choosing (A) and (f) properly. The optoelectronic feedback scheme has the advantage of ease of implementation, as it is insensitive to the optical phase of the output intensity. A comparison between unidirectional and mutual coupling, for the identical synchronization case when all the other control parameter are kept constant, revealed that while the first is extremely sensitive to deviations in The modulation feedback amplitude detuning, when the frequency is fixed to ($f=4$) the latter shows robust synchronization under identical operation

conditions and might be suitable for optical communication applications. From the above results we reveal that: In unidirectional coupling when ($a=0.4101$), This solution is stable and synchronization of the electric field and the carrier density in Master and Slave is accomplished and coherence function equal to ($C=0.98$ approach to 1) while in the mutual coupling when ($a=1.55$) and coherence function equal to ($C=1$) this is full synchronization in same equal Parameters, we note from the step of synchronization in mutual greater than unidirectional. We furthermore showed when the amplitude in unidirectional coupling ($a=0.4102$) it can be seen that after a short transient the two output signals become unsynchronized and coherence function equal to ($C=0.71$). But in the mutual coupling when ($a=1.5$) and the coherence function equal to ($C=0.8$). The detuning between amplitude of the two coupling configuration lasers plays a crucial role for identical synchronization. Even a small amplitude detuning prevents the lasers from synchronizing, as seen in partial synchronization, in unidirectional coupling we note that when ($a = 0.4098$) and coherence function equal to ($C = 0.75$) while in mutual coupling when ($a=1.56$) and coherence function ($C=0.96$) In this two coupling configuration, the coupling delay (ε) between the Master and the Slave, does not play any role in the synchronization process. Also we note that in the bidirectional coupling the synchronization is contentious between two oscillators in the range of amplitude ($0.158 > a > 11.61$) in our suggestion model while in the unidirectional configuration more sensitive than mutual coupling.

4.6 Recommendation

From this work we recommend that: The availability and ease of operation of diode lasers, in a wide range of configurations, make them a convenient test bed

for exploring basic aspects of nonlinear and chaotic dynamics. It also makes them attractive for practical tasks, such as chaos-based secure communications and random number generation. Avenues for future research and development of chaotic laser diodes are also identified. Also we Explained the variety of synchronized motion in coupled chaotic systems applications in both (unidirectional and mutual)configuration, for example it used to increase the power of lasers, to synchronize the output of electronic circuits, to control oscillations in chemical reactions or to encode electronic messages to secure communications.

Bibliography

- [1] Fischer, A.P., Andersen, O.K., Yousefi, M., Stolte, S. and Lenstra, D., (2000). "Experimental and theoretical study of filtered optical feedback in a semiconductor laser". "IEEE journal of quantum electronics", 36(3), pp.375-384.
- [2] Allaria, E., Arecchi, F.T., Di Garbo, A. and Meucci, R., (2001). "Synchronization of homoclinic chaos". "Physical review letters", 86(5), p.791.
- [3] Tang, S. and Liu, J.M., (2003). "Chaos synchronization in semiconductor lasers with optoelectronic feedback". "IEEE journal of quantum electronics", 39(6), pp.708-715.
- [4] Larger, L., Lacourt, P.A., Poinsot, S. and Hanna, M., (2005). "From flow to map in an experimental high-dimensional electro-optic nonlinear delay oscillator". "Physical review letters", 95(4), p.043903.
- [5] Sprott, J.C., (2007). "A simple chaotic delay differential equation". "Physics Letters A", 366(4), pp.397-402.
- [6] Arecchi, F. T., Meucci, R. and Gadomski, W., (1987). "Laser Dynamics with Competing Instabilities" "Physical Review Letters", 58, (2205).
- [7] Lu, K. and Wang, Q., (2011). "Chaotic Behavior In Differential equation Driven by A Brownian Motion" "Journal Of Differential Equation", 251, pp.(2853-2895).
- [8] Al-Naimee, K., Marino, F., Ciszak, M., Meucci, R. and Arecchi, F.T., (2009). "Chaotic spiking and incomplete homoclinic scenarios in semiconductor lasers with optoelectronic feedback". "New Journal of

Physics”, 11(7), p.073022.

[9] Li, Y., Wu, Z.M., Zhong, Z.Q., Yang, X.J., Mao, S. and Xia, G.Q.,(2014) .”Time-delay signature of chaos in 1550nm VCSELs with variable polarization FBG feedback”, ”Optics Express” 22, (19610-19620).

[10] Al-Naimee, K., Marino, F., Ciszak, M., Abdalah, S.F., Meucci, R. and Arecchi, F.T., (2010).” Excitability of periodic and chaotic attractors in semiconductor lasers with optoelectronic feedback”. ”The European Physical Journal D”, 58(2), pp.187-189.

[11] El-Dessoky, M.M. and Yassen, M.T., (2012). ” Adaptive feedback control for chaos control and synchronization for new chaotic dynamical system”.” Mathematical Problems in Engineering”, 2012.

[12] Flunkert, V., (2012).” Chaos synchronization in networks of delay coupled lasers: role of the coupling phases”. ” New Journal of Physics”,14(3),033039.

[13] Uchida, A., (2012),”Optical communication with chaotic lasers application and synchronization”, First edition, John Wiley and Sons.

[14] Zhang, J., Chung, H.S.H. and Lo, W.L., (2008). Chaotic time series prediction using a neuro-fuzzy system with time-delay coordinates. IEEE Transactions on Knowledge and Data Engineering, 20(7), pp. (956-964).

[15] Kantz, H. and Schreiber, T., (2004). Nonlinear time series analysis (Vol. 7). Cambridge university press.

[16] Camilleri, M., (2004), September. Forecasting using non-linear techniques in time series analysis: an overview of techniques and main issues. In Computer Science Annual Research Workshop (CSAW 2004), pp. (19-28).

[17] Wilding, R.D., (1998). Chaos theory: implications for supply chain management. The International Journal of Logistics Management, 9(1), pp. (43-

56).

[18] Addison, P.S., (1997). "Fractals and Chaos: an Illustrated Course", "CRC Press".

[19] Frazier, C. and Kockelman, K., (2004). "Chaos theory and transportation systems: instructive example". "Transportation Research Record:Journal of the Transportation Research Board", (1897), pp.(9-17).

[20] Wolf, A., Swift, J.B., Swinney, H.L. and Vastano, J.A.,(1985). "Determining Lyapunov exponents from a time series". "Physica D: Nonlinear Phenomena", 16(3), pp.285-317.

[21] Abraham, R. and Ueda, Y. eds., (2001). "The chaos avant-garde: Memories of the early days of chaos theory", (Vol. 39). "World scientific".

[22] Liu, Y. and Ohtsubo, J., (1994). "Experimental control of chaos in a laser-diode interferometer with delayed feedback". "Optics letters", 19(7), pp.(448 - 450).

[23] Mork, J., Tromborg, B. and Mark, J., (1992). "Chaos in semiconductor Lasers with optical feedback: theory and experiment". "IEEE Journal of Quantum Electronics", 28 (1), pp.93-108.

[24] Medrano-T, R.O., Baptista, M.S. and Caldas, I.L., (2005). "Basic structures of the Shilnikov homoclinic bifurcation scenario". "Chaos: An Interdisciplinary Journal of Nonlinear Science", 15(3), p.033112..

[25] Reich, D.S., Mechler, F., Purpura, K.P. and Victor, J.D., (2000). "Interspike intervals, receptive fields, and information encoding in primary visual cortex". "The Journal of neuroscience", 20(5), pp.(1964-1974).

[26] Fischer, I., Hess, O., Elser, W. and Gbel, E., (1994). "High-dimensional Chaotic dynamics of an external cavity semiconductor laser". "Physical review

letters”, 73(16), p.2188.

[27] Huguenii, C., Oscilatorium, H. and Muquet, A.F., (1986). Parisiis, 1673,”English translation: The pendulum clock”.

[28] Blekman,I.I.”Synchronization in Science and Technology”,(1981) (in Russian), Nauka, Moscow,(1988) (in English); ASME Press, NewYork.

[29] Fujisaka,H., and Yamada,T., Progress Theoretical Physics. (1983)[PTP](this is referred to as 1),69,32.

[30] Pecora, Louis M. and Carroll, Thomas L.,(1990). Journal of Physical Review Letter,”Synchronization in chaotic systems”64, (821-824).

[31] Rosenblum, M.G.,Pikovsky, A.S.,Kurths, J.,(1996),”Phase Synchronization of Chaotic Oscillators”,Journal of Physical Review Letters,76,1804.

[32] Rosa,E.R., Ott,E., Hess,M.H.,(1998),”Transition to phase synchronization of chaos”,Journal of Physical Review Letter,80,1642.

[33] Rosenblum,M.G. , Pikovsky,A.S., Kurths,J.,(1997)”From Phase to Lag Synchronization In coupled Chaotic Oscillators” Journal of Physical Review. Letter., 78, 4193.

[34] Rulkov,N.F.,Sushchik,M.M., Tsimring, L.S., Abarbanel,H.D.I.,(1995),” Synchronization of chaos in directionally coupled chaotic system”,journal of Physical. Review. E, 51, 980.

[35] Kocarev,L., Parlitz, U. (1996),”Generalized Synchronization, Predictability, and Equivalence of Unidirectionally Coupled Dynamical Systems”, journal of Physical. Review. letter, 76, 1816.

[36] Boccaletti, S., Valladares,D.L.,(2000)”Characterization of intermittent lag synchronization” journal of Physical. Review. E,62, 7497.

- [37] Zaks, M.A., Park, E.-H., Rosenblum, M.G., Kurths, J., (1999) "Alternating locking ratio in imperfect phase synchronization" *Journal of Physical Review Letters*, 82, 4228.
- [38] Femat, R. and Solis-Perales, G., (1999), On the chaos synchronization phenomena, "journal of Physical Review A", 262,(50-60)
- [39] Pikovsky, A.S., (1984), "On the interaction of strange attractors", "journal of Z. Physics. B- Condensed Matter", 55,(149-154).
- [40] Pecora, L.M., Carroll, T.L., (1991), "Driving systems with chaotic signals" *Journal of Physical Review A*, 44 ,2374.
- [41] Pecora, L.M., Carroll, T.L., (1990), "Synchronization in chaotic systems", *Physical Review Letters*, 64,(821).
- [42] He, R., Vaidya, P.V., (1992), "Analysis and synthesis of synchronous periodic and chaotic systems", *Journal of Physical Review A*, 46,(7387) .
- [43] Kapitaniak, T., (1994), "Synchronization of chaos using continuous control" *Journal of Physical Review E*, 50,(1642).
- [44] Amritkar, R.E., Gupte, N., (1993), "Synchronization of chaotic orbits: the effect of a finite time step" *Journal of Physical Review E*, 47,(3889).
- [45] Kocarev, L., Parlitz, U., (1995), "General Approach for Chaotic Synchronization with Applications to Communication", *Journal of Physical Review Letters*, 74,(5028).
- [46] Parlitz, U., Kocarev, L., Stojanovski, T., Preckel, H., (1996), "Encoding messages using chaotic synchronization" *Journal of Physical Review E*, 53,(4351).
- [47] Gmez, J., and Matas, M. A., (1995), "Modified method for synchronizing and cascading chaotic systems", *Journal of Physical Review E*, 52,(2145).

- [48] Wu, C.W. and Chua, L.O., 1994. A unified framework for synchronization and control of dynamical systems. *International Journal of Bifurcation and Chaos*, 4(04), pp.(979-998).
- [49] Carroll, T.L. and Pecora, L.M., (1993). Cascading synchronized chaotic systems. *Physica D: Nonlinear Phenomena*, 67(1-3), pp.(126-140).
- [50] Carroll, T.L., 1994. Synchronizing chaotic systems using filtered signals. *Physical Review E*, 50(4), p.2580.
- [51] Ohtsubo, J., (2008). "Semiconductor Lasers Stability, Instability and Chaos", Second, Enlarged Edition. *SPRINGER SERIES IN OPTICAL SCIENCES*, 111.
- [52] Rogister, F., Locquet, A., Pieroux, D., Sciamanna, M., Deparis, O., Mgret, P. and Blondel, M., (2001). "Secure communication scheme using chaotic laser diodes subject to incoherent optical feedback and incoherent optical injection". *Optics Letters*, 26(19), pp.(1486-1488).
- [53] Tang, S. and Liu, J.M., (2001). "Chaotic pulsing and quasi-periodic route to chaos in a semiconductor laser with delayed optoelectronic feedback". *IEEE journal of quantum electronics*, 37(3), pp.(329-336).
- [54] Solorio, J.S., Sukow, D.W., Hicks, D.R. and Gavrielides, A., (2002). "Bifurcations in a semiconductor laser subject to delayed incoherent feedback". *communications*, 214(1), pp.(327-334).